AD-A008 981

RESULTS OF AIRBLAST OVERPRESSURE MEASUREMENT PROGRAM AT PROJECT R. D. BAILEY

Michael J. Hoeft

Army Engineer Waterways Experiment Station
Livermore, California

February 1975

UNCLASSIFIED

SECURITY CLASSIFICATION OF THIS PAGE (When Data Entered)

REPORT DOCUMENTATION PAGE		READ INSTRUCTIONS BEFORE COMPLETING FORM
1. REPORT NUMBER MP E-75-4	2. GOVT ACCESSION NO.	3. RECIPIENT'S CATALOG NUMBER AD-A008 981
4. TITLE (and Subtitle) RESULTS OF AIRBLAST OVERPRESSURE MEASUREMENT PROGRAM AT PROJECT R. D. BAILEY		5. TYPE OF REPORT & PERIOD COVERED Final 6. PERFORMING ORG. REPORT NUMBER M E-75-4
7. AUTHOR(s) Michael J. Hoeft		8. CONTRACT OR GRANT NUMBER(s)
9. PERFORMING ORGANIZATION NAME AND ADDRESS U. S. Army Engineer Waterways Experiment Station Explosive Excavation Research Laboratory - Livermore, CA 94550		10. PROGRAM ELEMENT, PROJECT, TASK AREA & WORK UNIT NUMBERS Materials, Rock, Experimental Excavation Projects 31153
11. CONTROLLING OFFICE NAME AND ADDRESS		12. REPORT DATE February 1975 13. NUMBER OF PAGES 55
14. MONITORING AGENCY NAME & ADDRESS(if different from Controlling Office)		15. SECURITY CLASS. (of this report) UNCLASSIFIED 15a. DECLASSIFICATION/DOWNGRADING SCHEDULE

16. DISTRIBUTION STATEMENT (of this Report)

Approved for public release; distribution unlimited

17. DISTRIBUTION STATEMENT (of the abstract entered in Block 20, if different from Report)

18. SUPPLEMENTARY NOTES

19. KEY WORDS (Continue on reverse side if necessary and identify by block number)

Airblast overpressure
Airblast prediction
Blasting
Explosive excavation
Cratering
Explosives effects
Explosives

20. ABSTRACT (Continue on reverse side if necessary and identify by block number)

Methods of predicting gas-vent and ground-shock-induced airblast overpressure levels from underground explosions have been under investigation for many years. In order to obtain an accurate method for predicting peak overpressures and impulses from large-array-type detonations with different delay periods, more data from this type of event must become available. The airblast overpressure measurement program at R. D. BAILEY resulted in a large amount of data to be used, first, in estimating the airblast expected from future detonations in the R. D. BAILEY spillway area (continued)

DD FORM 1 JAN 73 1473 EDITION OF 1 NOV 65 IS OBSOLETE

UNCLASSIFIED

SECURITY CLASSIFICATION OF THIS PAGE (When Data Entered)

Item #20, abstract, continued

and, second, to provide further input to pred :tion method studies.

A discussion of the instrumentation and procedures used to obtain these data is followed by a presentation of the results and an analysis of these results. Since peak overpressures from various detonations were caused by several different airblast-producing mechanisms, no definite conclusions could be drawn concerning prediction methods. It is hoped that the results and their analysis can be used in future prediction method studies.

Destroy this report when no longer needed.
Do not return it to the originator.

The findings in this report are not to be construed as an official Department of the Army position unless so designated by other authorized documents.

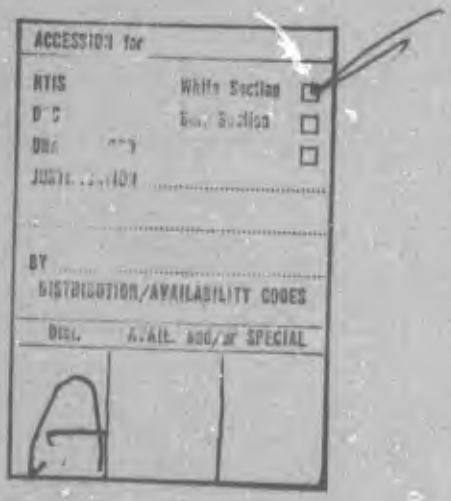

Printed in USA. Available from Defense Documentation Center,
Cameron Station, Alexandria, Virginia 22314 or
National Technical Information Service,
U. S. Department of Commerce
Springfield, Virginia 22161

TID-4500, UC-35
Peaceful Applications
of Explosives

MISCELLANEOUS PAPER E-75-4
RESULTS OF AIRBLAST OVERPRESSURE MEASUREMENT PROGRAM AT PROJECT R. D. BAILEY

Michael J. Hoeft

U.S. ARMY ENGINEER WATERWAYS EXPERIMENT STATION
EXPLOSIVE EXCAVATION RESEARCH LABORATORY
Livermore, California

MS. date, June 1974

1c

Preface

The U.S. Army Engineer Waterways Experiment Station (USAEWES) Explosive Excavation Research Laboratory (EERL) was the USAEWES Explosive Excavation Research Office (EERO) prior to 21 April 1972. Prior to 1 August 1971 the organization was known as the USAE Nuclear Cratering Group.

Project R. D. BAILEY was carried out by the USAEWES Explosive Excavation Research Laboratory in cooperation with the Huntington District. A summary report of this project, Project R. D. BAILEY Experimental Excavation Program, is presently being prepared for publication. The report presented here formed the basis for the airblast overpressure chapter of the summary report. It is presented in its entirety for reference and application to future studies.

COL E. D. Peixotto and COL G. H. Hilt were Directors of the Waterways Experiment Station and LTC R. R. Mills, Jr. was Director of EERL during the experimental excavation and the preparation of this report.

Abstract

Methods of predicting gas-vent and ground-shock-induced airblast overpressure levels from underground explosions have been under investigation for many years. In order to obtain an accurate method for predicting peak overpressures and impulses from large-array-type detonations with different delay periods, more data from this type of event must become available. The airblast overpressure measurement program at R. D. BAILEY resulted in a large amount of data to be used, first, in estimating the airblast expected from future detonations in the R. D. BAILEY spillway area and, second, to provide further input to prediction method studies.

A discussion of the instrumentation and procedures used to obtain these data is followed by a presentation of the results and an analysis of these results. Since peak overpressures from various detonations were caused by several different airblast-producing mechanisms, no definite conclusions could be drawn concerning prediction methods. It is hoped that the results and their analysis can be used in future prediction method studies.

Acknowledgments

This report is based on the work of Hudson Washburn of the Explosive Excavation Research Laboratory (EERL), who planned and executed the airblast overpressure measurement program at Project R. D. BAILEY. Lymon Watson and James Tarver of the Instrumentation Services Division, WES, assisted with the program. Many people of EERL provided valuable assistance during the project and in the writing of this report: Thomas Tami, William Bechtell, Project Technical Deputy, Richard Fraser and MAJ George Miller, Project Test Managers, John Shaler, Project Engineer, and Stephen Kelley, Kenneth Crichton, Mathew Zahn, and Richard Gerbino

Contents

FIGURES

FIGURES (continued)

TABLES

TABLES (continued)

Conversion Factors

British units of measurement used in this report can be converted to metric units as follows:

Multiply	By	To obtain
inches	2.54	centimeters
feet	0.3048	meters
cubic feet	0.02832	cubic meters
cubic yard	0.764555	cubic meters
pounds	0.4535924	kilograms
pounds per cubic foot	16.02	kilograms per cubic meter
Fahrenheit degrees	5/9	Celsius or Kelvin degrees[a]

[a]To obtain Celsius (C) temperature readings from Fahrenheit (F) readings, use the following formula: $C = (5/9)(F - 32)$. To obtain Kelvin (K) readings, use: $K = (5/9)(F - 32) + 273.15$.

RESULTS OF AIRBLAST OVERPRESSURE MEASUREMENT PROGRAM AT PROJECT R. D. BAILEY

Introduction

Airblast overpressure is an explosion effect capable of causing damage at locations well beyond the detonation site. Predictions of this effect are necessary to determine the probability of damage occurring at various distances from explosions of various sizes and designs.

PURPOSE AND SCOPE

In order to refine further the present prediction methods, data must be available from detonations that contain variables that have not yet been adequately accounted for. Such variables include (1) the effects of quarry walls, intervening hills, or vegetation on the airblast pulse, (2) the errors involved in considering the depth of burial of large length-to-diameter ratio charges to be at the center of the charge, and (3) the expected enhancement in various directions of various charge configurations and delay sequences.

Because each detonation at R. D. BAILEY contained all these variables, it was hard to isolate the effect from any one of them. Still, it is hoped that the presentation of the data obtained from this project along with the analysis of the data can be used in conjunction with future experimental data to define further the expected results from time-delayed multicharge array detonations.

To help in understanding the data and its analysis, a background description of airblast is presented, followed by an explanation of what was involved in obtaining the data.

PROJECT DESCRIPTION

Project R. D. BAILEY was an experimental excavation program conducted on the site of the spillway for the R. D. BAILEY Dam near Justice, West Virginia. Its purpose was to determine an effective and economical method of excavation for the spillway and at the same time to provide acceptable material for use as fill in the dam itself. For this reason the program was designed to test various blast hole diameters and depths, burdens, spacings, delays, and explosives types. To do this, a series of test blasts were designed, each one containing one or more variables different from those of the preceding one. These pilot blasts were numbered and given the prefix "PB." In some cases a presplit line was detonated several hours before the main charges. These were indicated as "PB-4 presplit," etc.

In addition to the practical applications, this program also provided much useful scientific data on blasting techniques and effects. Among these technical programs were the fragmentation program, subsurface

velocity and blast-induced fracturing program, seismic motion program, photography program, and airblast overpressure measurement program.

Background

In order to discuss the airblast overpressure measurement program implemented at R. D. BAILEY, it is necessary to have an understanding of just what airblast overpressure is, what has been done with it in the past, and how results of past programs have been correlated to form current standards.

THEORY

There are two primary mechanisms responsible for producing airblast pressure waves (also called airblast pulses or airblast overpressure) from a subsurface explosion: ground-shock-induced overpressure, and gas-vent-induced overpressure.* Ground-shock-induced overpressure results when the initial stress wave from the explosion reaches the surface and causes spalling. This spalling compresses the air above, much like a piston, producing a region of higher pressure that travels away in a wave-like manner. Gas-vent-induced overpressure will occur when the expanding gases from the explosion vent through the dissociating mound, creating a pressure wave that travels outward. However, if the explosives are deeply buried, such as in mounding or contained detonations, the expanding gases will be at or near ambient atmospheric pressure by the time they vent so that their contribution to the airblast wave will be negligible. A typical airblast overpressure trace containing these two pulses is shown in Fig. 1. This would be the type of trace expected from a single-charge detonation.

For detonations containing more than one charge, such as a row or array of charges, it is quite possible that the waves from different charges will combine to produce a resultant wave different in amplitude and shape from the single-charge pulses. If, in addition, there are delays between some of the charge detonation times, the degree of combination of airblast waves from different charges will depend on both the delay times and the charge separation distances, and the relative relationship of these two parameters will depend on the location of the point of interest with respect to the charges.

These airblast waves from subsurface explosions may also be enhanced or sometimes completely overshadowed if surface primacord is used to detonate the charges. Whereas the airblast wave produced by a single subsurface charge is considered a hemispherical wave, the pressure wave from an extended primacord line should be considered a cylindrical wave at short distances from the detonation site. At distances much

*Other mechanisms that cause positive airblast pulses are the ground-transmitted ground-shock-induced pulse, the surface Rayleigh-wave-induced pulse, and the positive restoration pulse. These pulses may appear on overpressure records, but they are small enough to be considered unimportant in airblast safety considerations. [1]

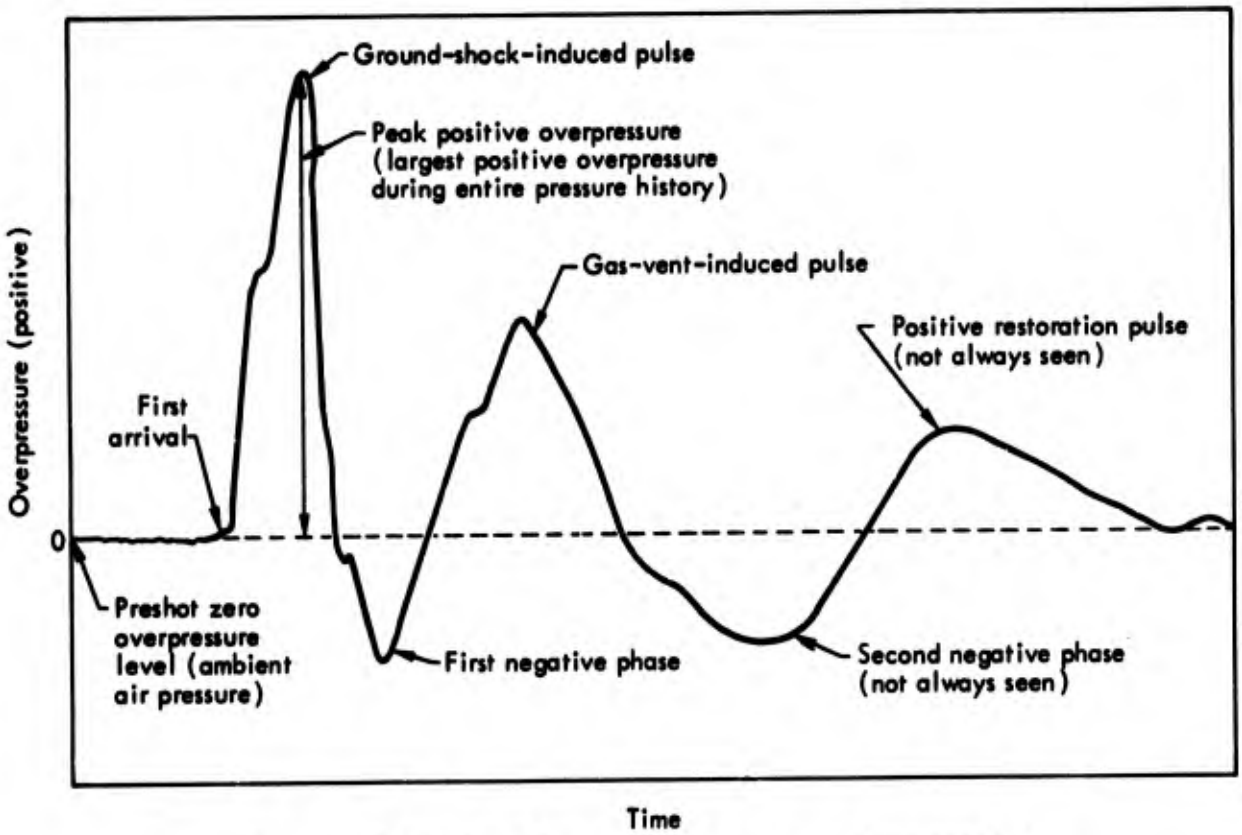

Fig. 1. Typical airblast overpressure-vs-time record.

greater than the length of the primacord, however, the wave can also be considered hemispherical. At any rate, the effect on wave combination of multiple rows of primacord and the dependence of this effect on separation distances and delay times should be similar to that for multiple charges.

As the pulses from subsurface charges and primacord combine and travel outward, the propagation rate will be affected by both atmospheric and geographic conditions in the area. The propagation rate will increase in the downwind direction and also in the direction of increasing temperature.[2] A mountain, hill, or other steep surface will tend to deflect the wave upward. A combination of the above could tend to focus the overpressure in a particular direction causing annoying sonic disturbances as well as structural damage and injury to personnel.

HISTORY

Previous EERL experience in airblast measurement has come primarily from single-charge and a few simple row- and array-charge detonations. Since most of these detonations were experiments designed to provide explosives effects data, they produced quite well-defined airblast wave pulses, and peak levels were usually accurately predictable.

Since the detonations at Project R. D. BAILEY were designed for determination of effective quarrying configurations and not necessarily for explosives effects data, many variables were present that had not been encountered simultaneously in past experiments. These included a variety of

charge sizes and length-to-diameter ratios, array configurations, initiation mechanisms, delay patterns, explosives types, and local topographic and geologic features. How the uncertainties introduced by so many variables were handled will be discussed later.

CURRENT STANDARDS

At present, the two properties of an airblast pulse believed to be important when damage is considered are peak positive overpressure and impulse.

In the past it was generally believed that peak positive overpressure was of most importance in anticipating damage. Numerous studies have related measured overpressure to observed damage.[3-5] The results of two such studies are shown in Fig. 2. The left side of this figure was adapted from Ref. 2, and the right side from Ref. 5. There are many reasons

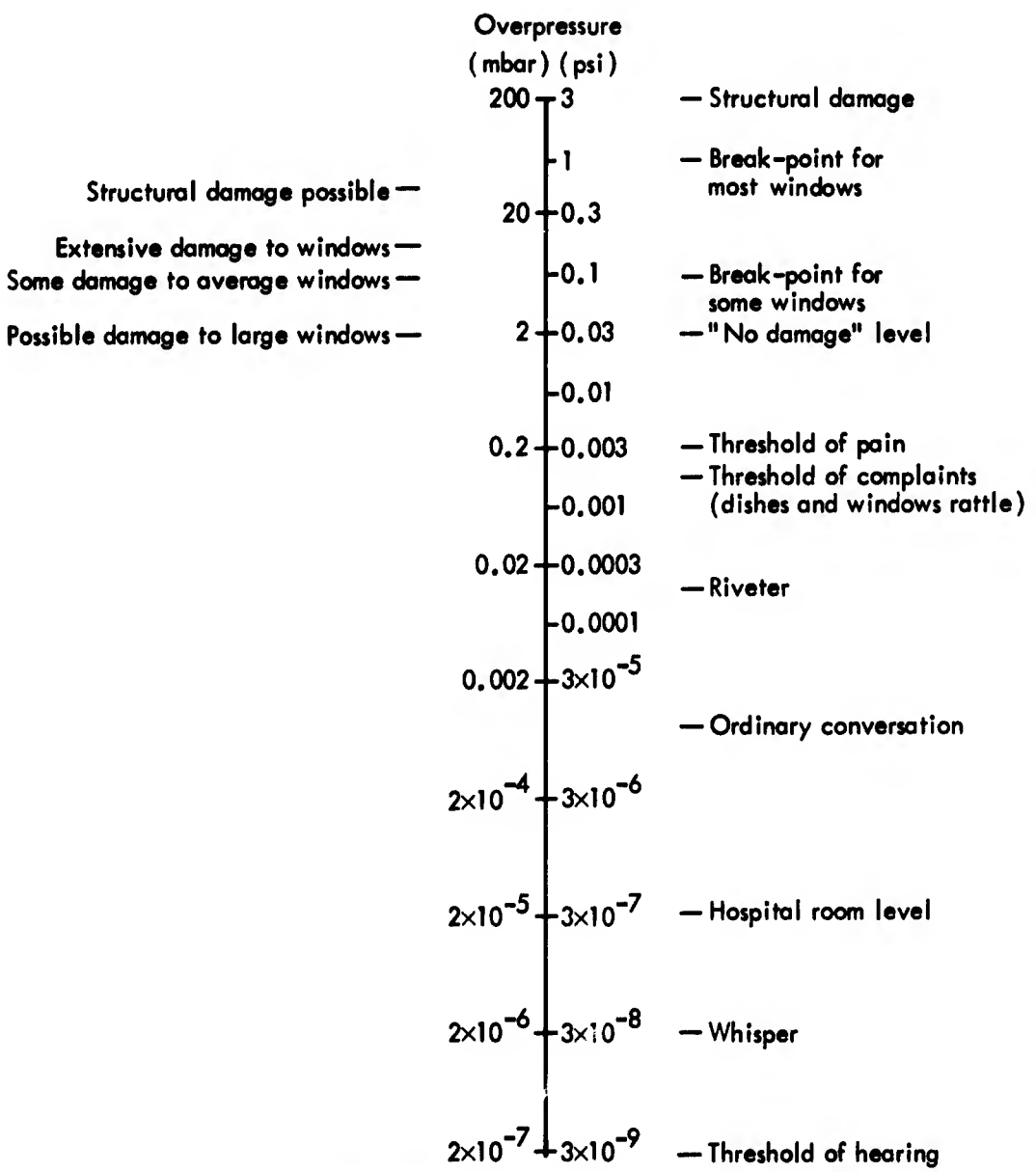

Fig. 2. Airblast damage criteria (adapted from Refs. 2 and 5).

for the differences in the two sides. Data were obtained from different experiments and different explosives types and configurations. In addition, windows are naturally difficult to categorize due to differences in size and thickness, quality of glass, age of glass, stress conditons introduced during framing, and stress conditions introduced by differential solar heating at the time of test. The standards on the left side of Fig. 2, besides being more conservative, are believed, from the experience of EERL personnel, to be more accurate.

Recently, consideration has been given to the importance of impulse in causing damage. Whereas peak overpressure gives the maximum pressure to which a window is subjected, impulse gives the length of time a window is subjected to a certain pressure. (It is defined as the time integral of the air-blast overpressure.) To date, however, there has not been enough research in this area to yield precise standards for general application.

Airblast Measurement Program

EXPERIMENTAL OBJECTIVES AND APPROACH

The object of Project R. D. BAILEY pilot spillway excavation was, among other things, to provide technical information useful as guidelines for specifications in the main contract for the spillway excavation. Because airblast is a potential hazard to personnel and structures near subsurface explosions, an airblast measurement program was initiated to determine the form and amplitude of airblast pressure waves produced by the experimental explosions, and to correlate these data with previously established damage criteria. An analysis of the results from all the experiments was then to be used to establish a prediction procedure whereby damage probability levels at various distances could be determined for similar types of production blasting in the R. D. BAILEY Lake spillway area. In this way, certain criteria might be established that could define the size and pattern design limits that had a substantial probability of damaging nearby objects by excessive airblast overpressures.

Project R. D. BAILEY provided an opportunity to obtain airblast information from explosive charges in a conventional excavation mode. Since there is a lack of systematic airblast measurements and analyses for these types of explosions, the results of such a program could help fill that gap and could be useful in airblast predictions for future similar explosive excavation applications.

In summary, the objectives of the airblast technical program were essentially twofold:

1. To provide technical input to the main contract for the R. D. BAILEY Lake spillway excavation

2. To provide airblast data and analyses of that data that would extend the understanding of airblast production in quarry-type blasting

The approach taken to attain these objectives is described below.

In order to provide input to the R. D. BAILEY contract, it was necessary to

determine airblast levels that could be expected in areas in which people or structures might be exposed to damaging airblast overpressures. Therefore, airblast measurements were taken at the site of the future intake structure for the dam (approximately 2000 ft south of the project area), and in the town of Justice (approximately 1 mi southwest of the project area).

To provide useful data for the analysis of the effects of the many variables present, the following steps were taken. Because of the varying terrain features in the area, measurements were taken in several directions in hopes of determining the effects of these features. Since each successive shot was located beneath the previous one, a high wall gradually formed on three sides of the detonation site. Thus, measurements were needed in the direction of the open end as well as one or more of the other directions in order that the effects of wall height could be ascertained. Finally, to determine airblast variance with distance, several measurements were needed at increasing distances in each of the chosen directions.

INSTRUMENTATION

To record adequately the airblast records from all shots at R. D. BAILEY, eight airblast gages were used. These gages were Dynasciences Model P7D variable reluctance differential pressure transducers. One side of each gage was open to the atmosphere while the other side was equipped with a damping tube designed to allow only low frequency changes in the ambient atmospheric pressure to be equalized on both sides of the gage.

Six of the airblast gages were "hard-wired" to the Control Point trailer using Belden four-conductor-shielded cable. These gages were part of a 3-kHz ac bridge, the output of which was demodulated, amplified, and recorded on both a 12-in. 36-channel oscillograph and a 14-channel tape recorder. On both of these were also recorded an IRIG B* time code signal and breakwire-derived detonation time pulses. The IRIG B time code signal is a 1-kHz sinusoidal signal with two amplitudes that are patterned to code the exact data and time to a millisecond, providing an accurate time base. The detonation time signal is derived from a breakwire wrapped around the primacord or detonation cap and given an accurate time of detonation for each delay period. The airblast recording system is depicted in modular form in Fig. 3.

The use of both an oscillograph and tape recorder provided a means of using different sensitivities in recording a data channel and also furnishing backup recording protection. The paper record provided the initial field-reduced data, and the tape record was to be digitized and analyzed by computer.

The remaining two gages were operated from what were called "remote units." These are essentially a 5-kHz ac bridge with demodulator and amplifiers with outputs for either a voltage measuring recorder or a current measuring device, such as an oscillograph. One of the remote units was recorded on a Sanborn pen recorder, and one on a Honeywell

*Inter-Range Instrument Group standard B.

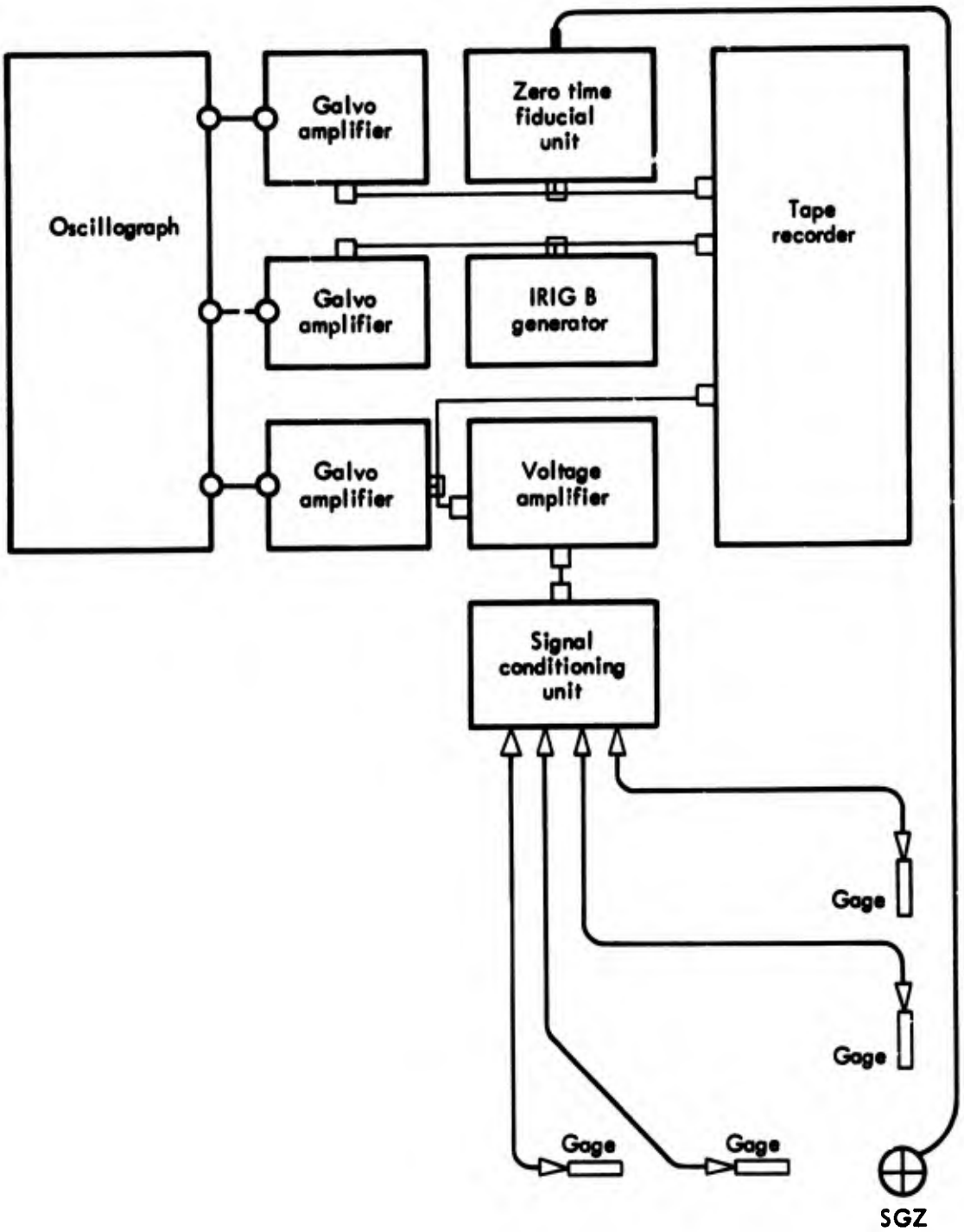

Fig. 3. Modular airblast system (generalized).

Visicorder oscillograph. No detonation times or IRIG B time code were recorded at these stations.

A detailed list of specifications for this system is given in Appendix A.

PROCEDURE

The procedure used in the field to obtain sufficient airblast data to satisfy the experimental objectives included

locating, setting up, and maintaining the gages, predicting peak overpressures expected from each shot, and recording the data on shot day.

Gage Location, Setup, and Maintenance

As stated previously, the plan was to use gages in various directions as well as distances from the detonation area. Therefore, the eight gages were located in three principal directions from the detonation site. Three gages were placed at different distances in the easterly direction roughly along the center line. These gages were perpendicular to the axis of the rows of charges, and they always had a clear view of the detonation area, because the eastern end of the excavation was always open. The view from the western side, however, was blocked by a wall that increased in height as the project progressed. Three gages (including one in Justice) were placed at different distances in the westerly direction to measure the effect of this wall, as well as the effect of different topographic conditions. The remaining two gages (including one at the site of the intake structure) were placed perpendicular to the center line in a southerly direction to measure the airblast off the ends of the rows of charges as well as to give additional information on increasing wall height and varying topographic conditions. All these gage locations are shown in plan view in Fig. 4 with a simplified cross-sectional view in Fig. 5.

These gages were originally placed so as to have as clear a view of the shot area as possible. During the course of the project it sometimes became necessary due to changes in the natural surroundings or the geometry of the excavation, to move a gage from its original position. All gage positions were surveyed for both horizontal coordinates and elevation. These data, along with the position of each gage relative to the spillway center line, are tabulated in Table 1.

Because terrain features made access to some of the gage locations difficult, it was decided to leave the gages in position for the duration of the project to expedite shot-day procedures. This decision necessitated precautions to insure that gages would not be moved or damaged by extreme weather conditions. For this reason each gage and damping tube assembly was mounted on a board and secured to the ground or a tree. It was then covered with a plastic tent that was open at both ends to allow the airblast pulse to pass through without being altered in the immediate vicinity of the gage. This assembly is illustrated in Fig. 6.

The six gages that were wired directly to the control point trailer were checked daily for possible damage to the cable or the gage itself. This was usually a continuity check from the trailer. If a problem was discovered on one of the channels, a visual check of the gage and cable was made. It was usually found that problems in this area were caused by one of two things: either the cable was gnawed through by rodents, or moisture had accumulated in the cable connectors. The first problem could be avoided by hanging the cable in trees or bushes where possible, and the second, by covering the connectors with plastic, which kept off outside moisture and allowed air to circulate to dry any condensation.

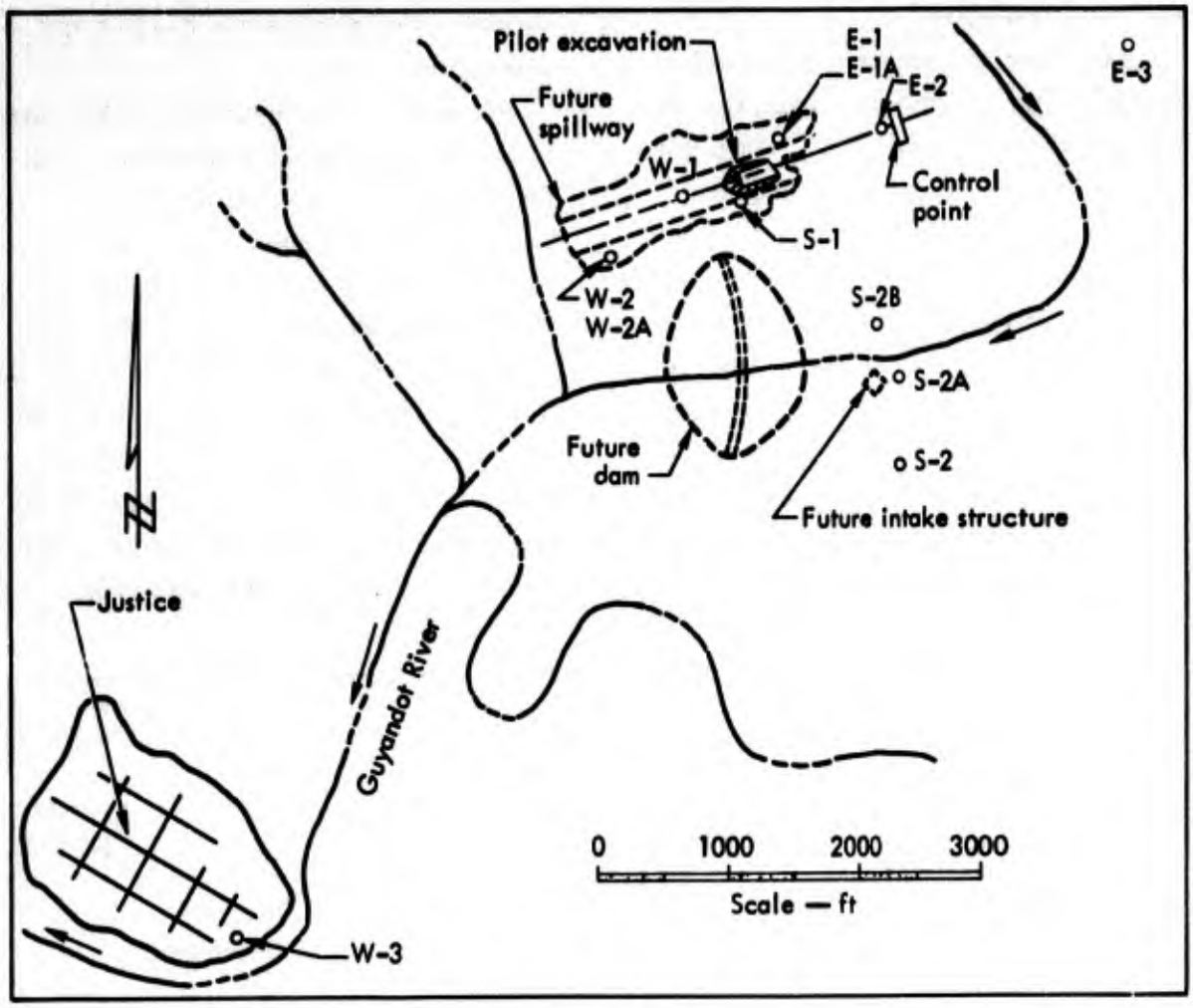

Fig. 4. Plan view of airblast gage locations.

Prediction Method

Because of the many variables involved in the detonations for this project as compared to previous work, existing prediction methods were considered insufficient. Therefore, the predictions obtained by means of the methods described in Ref. 6 were used only as a starting point. These predicted values were then adjusted by means of expected intercharge and inter-row reinforcement factors as determined by delay times and charge separations. A suppression factor was then applied to account for the expected effect of intervening hills, trees, and quarry wall in the different directions. For the first few shots, these factors were estimated by conservative guesses. The results of these early shots were then used to estimate factors for subsequent shots.

Reference 7 provides another method for predicting peak overpressure. However, because this prediction method considers only the maximum charge weight detonated per delay interval, it was considered inadequate to predict possible inter-row reinforcement. As a result, predictions based on Ref. 7 were not made prior to the R. D. BAILEY blasts.

Shot-Day Procedure

On the day of each shot, continuity to all gages was again checked and cables repaired if necessary. The appropriate calibration resistors (determined by predictions) were inserted so as to give a known voltage level that would correspond roughly with the expected peak airblast overpressure voltage. This voltage level was recorded on both the oscillograph and the tape recorder at approximately 2 min before detonation and again at 2 min after detonation. Also recorded were the temperature and general weather conditions at the time of the detonation.

All data recordings were in the form of a time history of the pressure monitored at each gage from about 3 sec before the detonation time to several seconds after detonation. The recorders were turned on and off manually. The tape recorder and the oscillograph at the Control Point were run at 7-1/2 in./sec and 40 in./sec, respectively, and the remote units were recorded at 100 mm/sec and 50 in./sec for the pen recorder and the oscillograph, respectively.

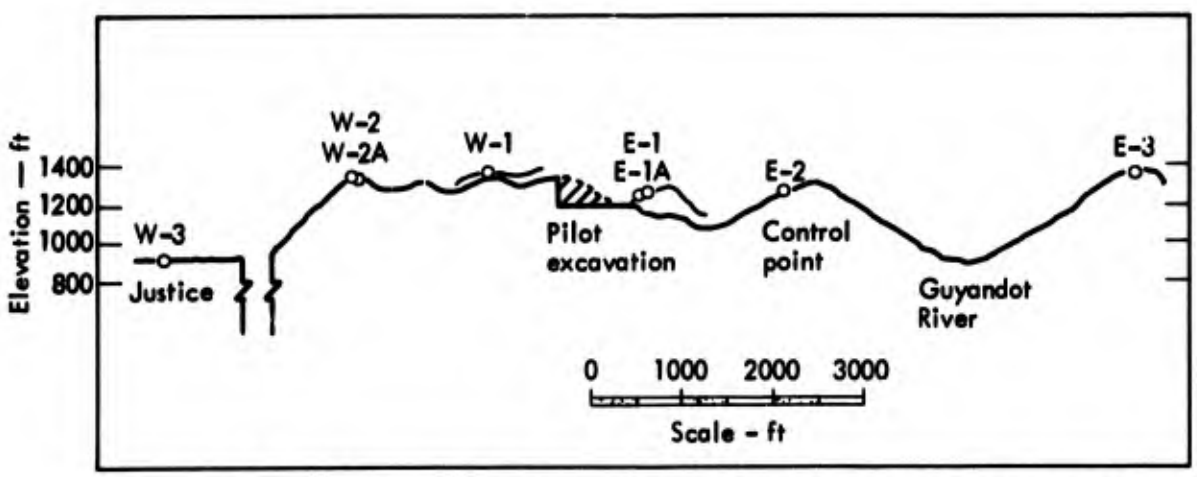

(a) E-W section approximately parallel to spillway center line (looking north).

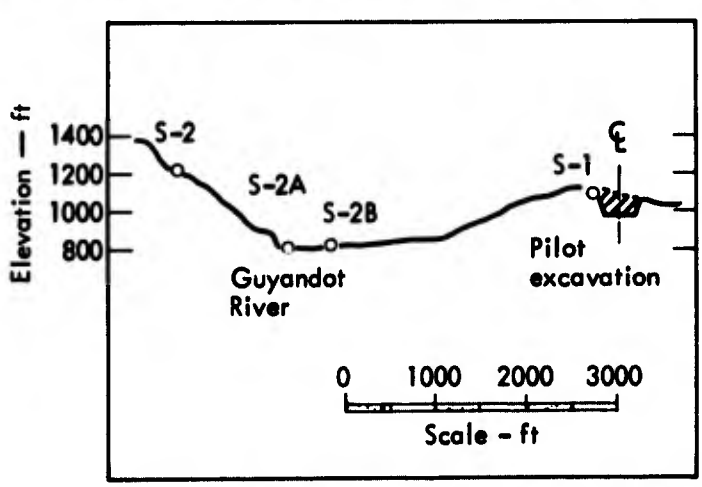

(b) N-S section approximately perpendicular to spillway center line (looking west).

Fig. 5. Topographic profiles through airblast gage locations.

Table 1. Airblast gage locations.

Gage	Coordinates North	Coordinates East	Elevation (ft)	Referenced to spillway center line Station	Referenced to spillway center line Offset (ft)
W-1	220,506	1,761,196	1373	12+29	2 left
W-2	220,080	1,760,613	1338	19+13	233 left
W-2A	220,079	1,760,608	1343	19+18	232 left
W-3	215,122	1,757,719	890	61+65	4090 left
E-1	220,915	1,761,915	1255	4+20	172 right
E-1A	220,912	1,761,908	1243	4+28	171 right
E-2	220,982	1,762,737	1269	-3+84	12 left
E-3	221,625	1,764,586	1349	-23+41	45 right
S-1	220,467	1,761,602	1304	8+53	161 left
S-2	218,525	1,762,859	1413	2+39	2392 left
S-2A	219,164	1,762,884	910	0+23	1790 left
S-2B	219,555	1,762,700	920	0+81	1361 left

(a) Gage and damping tube on mounting board

(b) Gage assembly under protective tent

Fig. 6. Airblast gage assemblies.

Results

The results of the airblast data collection effort are listed in Table 2. The gage locations listed correspond with those illustrated in Figs. 4 and 5. Because the velocity of an airblast pulse corresponds roughly with that of sound (approximately 1087 ft/sec), it would be expected that the time (in seconds) of first pulse time-of-arrival (TOA) would be approximately equal to the distance of the gage from the charges multiplied by 10^{-3}. As can be seen, the TOA is less than this value in all cases – due to the fact that the pulse does not radiate from

Table 2. Measurement of peak positive overpressure.

Shot	Gage	Approximate distance from SGZ (ft)	Time of first pulse arrival (sec)	Peak positive overpressure (psi)
PB-1	W-1[a]	350	0.273	0.187
	W-2	1050	0.905	.0038
	W-3	6000	—[b]	.0013
	S-1	160	0.113	.0668
	S-2	1500	—	.0026
	E-1	500	0.433	.0386
	E-2	1350	1.124	.0368
	E-3	3300	2.878	.0200
PB-2 presplit	W-1	300	0.298	.138
	W-2	1100	0.930	.0155
	W-3	5940	—	—[c]
	S-1	100	0.086	.152
	S-2	2000	—	.0035
	E-1	500	0.444	.0316
	E-2	1300	1.165	.0616
	E-3	3300	2.928	.0182
PB-3 buffer zone	W-1	368	0.342	.0247
	W-2A	1087	0.970	.00236
	W-3	6000	—	.00063
	S-1	150	0.115	.0315
	S-2	2300	—	.00107
	E-1	465	0.407	.0190
	E-2	1244	1.090	.0184
	E-3	3300	2.812	.0042
PB-3	W-1	408	0.388	.0428
	W-2A	1127	1.042	.0116
	W-3	6000	—	.0026
	S-1	160	0.158	.0995
	S-2	2 00	—	.0061
	E-1	425	0.377	.0845
	E-2	1204	1.066	.0220
	E-3	3200	2.781	.00755
PB-4 presplit	W-1	480	0.360	.0443
	W-2A	1200	0.981	.00406
	W-3	6000	—	.00036
	S-1	150	0.085	.110
	S-2	2300	—	.0069
	E-1	370	0.317	.061
	E-2	1200	0.941	.0571
	E-3	3220	2.687	.0168
PB-4	W-1	480	0.459	.059
	W-2A	1200	1.075	.0107
	W-3	6000	—	.00108
	S-1	150	0.180	.0935
	S-2	2300	—	.0087
	E-1	370	0.263	.121
	E-2	1200	0.862	.0302
	E-3	3220	2.588	0.0060

Table 2 (continued)

Shot	Gage	Approximate distance from SGZ (ft)	Time of first pulse arrival (sec)	Peak positive overpressure (psi)
PB-4A	W-1	540	0.577	0.0266
	W-2A	1290	1.107	.0094
	W-3	6000	–	.00217
	S-1	240	0.196	.238
	S-2	2300	–	.0070
	E-1	325	0.245	.145
	E-2	1090	–	–
	E-3	2750	2.622	.00388
PB-4B,C	W-1	480	0.397	.102
	W-2A	1240	1.005	.032
	W-3	6000	–	.0024
	S-1	200	0.125	.179
	S-2	2300	–	.0149
	E-1	380	0.249	.165
	E-2	1134	0.867	.0175
	E-3	2800	–	–
PB-4D	W-1	480	0.403	.0252
	W-2A	1240	1.034	.00477
	W-3	6000	–	.00123
	S-1	200	0.176	.0915
	S-2	2300	–	.00695
	E-1	380	0.288	.113
	E-2	1134	0.964	.0220
	E-3	2800	2.683	.00431
PB-5	W-1	655	0.633	.0212
	W-2A	1400	1.251	.00346
	W-3	6000	–	.000891
	S-1	300	0.316	.0324
	S-2	2300	–	.00572
	E-1	260	0.206	.2205
	E-2	960	0.795	.0386
	E-3	3000	2.522	.00649
PB-4E	W-1	440	0.401	.00434
	W-2A	1200	1.032	.00590
	S-1	220	0.216	.096
	S-2B	1700	–	.0086
	S-2	2500	–	.0070
	E-1A	370	0.306	.0887
	E-2	1180	1.019	.0279
	E-3	3000	2.736	.00688
PB-6A presplit	W-1	620	0.499	.0382
	W-2A	1360	1.110	.00596
	W-3	–	–	–
	S-1	260	0.167	.0448
	S-2	2300	–	.00285
	E-1	300	0.230	.0855
	E-2	1000	0.856	.0299
	E-3	2800	2.578	0.00451

Table 2 (continued)

Shot	Gage	Approximate distance from SGZ (ft)	Time of first pulse arrival (sec)	Peak positive overpressure (psi)
PB-6A	W-1	600	0.521	0.059
	W-2A	1330	1.135	.0102
	S-1	250	0.217	.161
	S-2A	1800	–	.0067
	S-2	2400	–	.0153
	E-1	300	0.224	.37
	E-2	1020	0.827	.058
	E-3	3000	2.553	.0121
PB-6B	W-1	520	0.400	.0662
	W-2A	1270	1.016	.0125
	S-1	200	0.050	.104
	S-2A	1800	–	.0231
	S-2	2400	–	.0279
	E-1A	340	0.188	.182
	E-2	1100	0.853	.0738
	E-3	3000	2.576	.0154
PB-6C	W-1	520	0.443	.0271
	W-2A	1270	1.057	.00123
	S-1	200	0.172	.0410
	S-2A	1800	–	.00734
	S-2	2400	–	.00378
	E-1A	340	0.245	.128
	E-2	1100	0.909	.0196
	E-3	3000	2.635	.00304
PB-7	W-1	530	0.467	.0402
	W-2A	1290	1.101	.0123
	W-3	6000	–	.00187
	S-1	250	0.207	.0959
	S-2	2480	–	.0114
	E-1A	300	0.170	.171
	E-2	1080	0.858	.0615
	E-3	3000	2.583	.0133
PB-8	W-1	450	0.403	.0107
	W-2A	1200	1.024	.00905
	W-3	6000	–	.00512
	S-1	180	0.130	.306
	S-2	2450	–	.0188
	E-1A	390	0.300	.336
	E-2	1160	1.004	.113
	E-3	3110	2.743	0.0222

[a]See Figs. 4 and 5 for relative locations and elevations.

[b]Blanks in this column indicate remote units that did not have usable time record capabilities.

[c]Blanks in this column indicate loss of data due to system malfunction.

a single point source but from an array of sources; yet the distances were estimated to the approximate center of the array. Also, the airblast pulse travels at supersonic velocities over a portion of the distance between the charges and the gage locations – a fact that causes smaller measured TOA values.

The data obtained from the two remote stations did not contain the IRIG B time code plots as did the data from the six gages recorded at the Control Point trailer; therefore, the TOA for these two gages could not be accurately established. This fact explains the blanks in the TOA column.

The four blanks that occur in the peak positive overpressure column occurred due to system malfunctions. It should be noted that this loss of data did not occur on any of the eight main production detonations. In fact, of the 136 possible overpressure measurements, usable data were obtained from 132 of them.

Appendix B presents plots of overpressure as a function of time for several selected gage locations. These plots show the type of airblast generated by many of the test blasts.

Appendix C contains plots of the data from Table 2 (overpressure vs distance) for each shot.

Analysis

The airblast overpressure data were reduced by computer to obtain plots of peak positive overpressure, impulse, energy Fourier amplitude, and phase angle for each channel of data from every shot. The following is an analysis of the relation of overpressure and impulse data for the various shots followed by a discussion of the effectiveness of prediction procedures.

PEAK POSITIVE OVERPRESSURE

Table 3 is a summary of the peak airblast overpressures for most of the excavation detonations. This table was developed as follows:

The data from the gages along the center line in the direction looking east from the shot area were used to obtain a fit to those data from which the peak pressure at 1000 ft in that direction was obtained by interpolation. This is the peak overpressure ($\Delta P\text{-}E_{1000}$) value indicated. The fit to these points did not

Table 3. Summary of peak airblast overpressures.

Shot	Total yield (lb)	LSY[a] (lb)	Slope b (r^{-b})	$\Delta P\text{-}E_{1000}$ (psi)
PB-1	1,150	260	0.7	0.044
PB-3	3,380	3,380	1.1	.027
PB-4	20,000	4,000	1.5	.036
PB-4PS	–	–	1.3	.075
PB-4A	803	–	1.6	.021
PB-4B&C	4,811	–	1.7	.023
PB-4D	1,581	–	1.6	.026
PB-5	1,188	258	1.5	.037
PB-6APS	–	–	1.5	.030
PB-6A	15,350	2,868	1.5	.050
PB-4E	550	–	1.4	.032
PB-6B	8,600	3,993	1.5	.082
PB-7	19,950	3,700	1.2	.067
PB-8	32,100	10,990	1.4	0.14

[a]LSY – largest simultaneous yield, which is the largest amount of explosives detonated during one time delay.

exhibit the same distance dependence for each shot (r^{-b}) because the slope "b" of the fitted line actually varied from about 0.7 to 1.7, although most were approximately 1.5. This high amplitude decay rate is indicative of small charges that produce short duration pulses. (Appendix C contains plots of the peak positive overpressures vs distance for each shot, from which the $\Delta P\text{-}E_{1000}$ values were obtained.)

The $\Delta P\text{-}E_{1000}$ was plotted as a function of total yield and largest simultaneous yield in Figs. 7 and 8, respectively. Although the general trend is an increasing overpressure with increasing yield, the points of Figs. 7 and 8 are so scattered that no definite conclusions can be drawn from them insofar as predicting overpressure from a given total yield or largest simultaneous yield is concerned. From a study of the data, it appears that this scatter can be explained by the fact that, instead of being caused by intercharge enhancement of ground-shock-induced pulses as expected, peak positive overpressures for most detonations appear to have been caused by three other mechanisms: detonating cord spikes, single-hole stemming failures, and gas-vent-induced pulses. These three mechanisms are described below.

Ideally, because of the design of the arrays, it was expected that the peak positive overpressures were caused by ground-shock-induced pulses from adjacent holes and rows combining to create a larger pulse. When this combining occurs, the resulting record is a series of short pulses that add up to give the general appearance of a wave with a fairly long positive phase followed by a slightly longer negative phase. This wave is apparent in Fig. 9, which shows

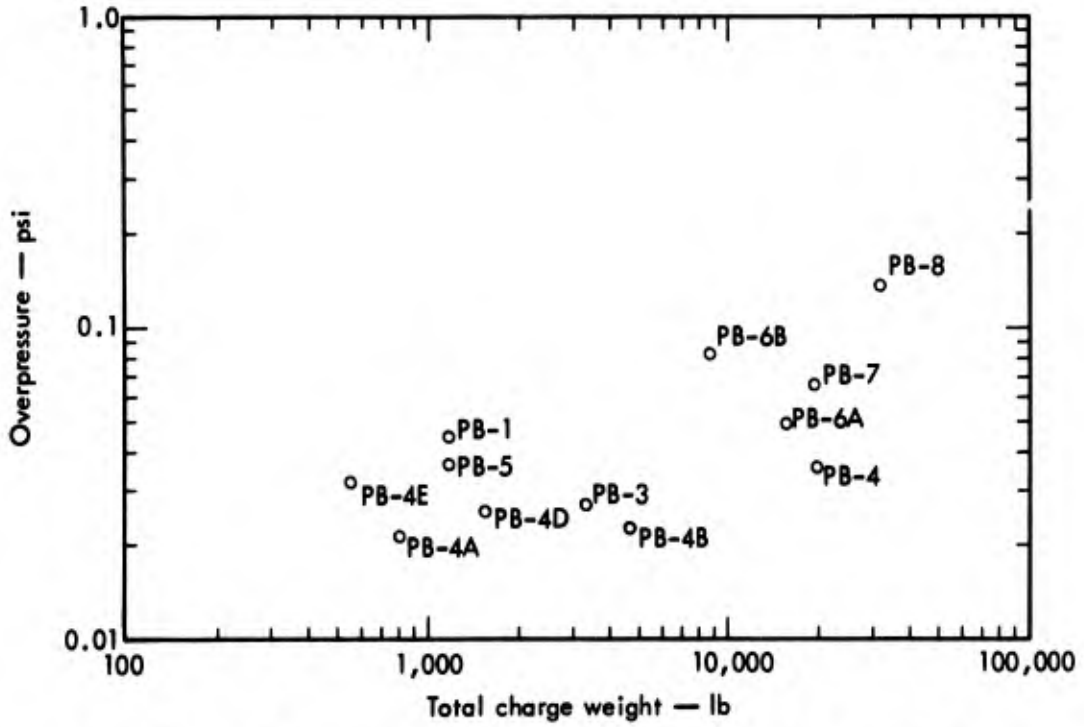

Fig. 7. Peak overpressure vs total charge weight at 1000 ft east.

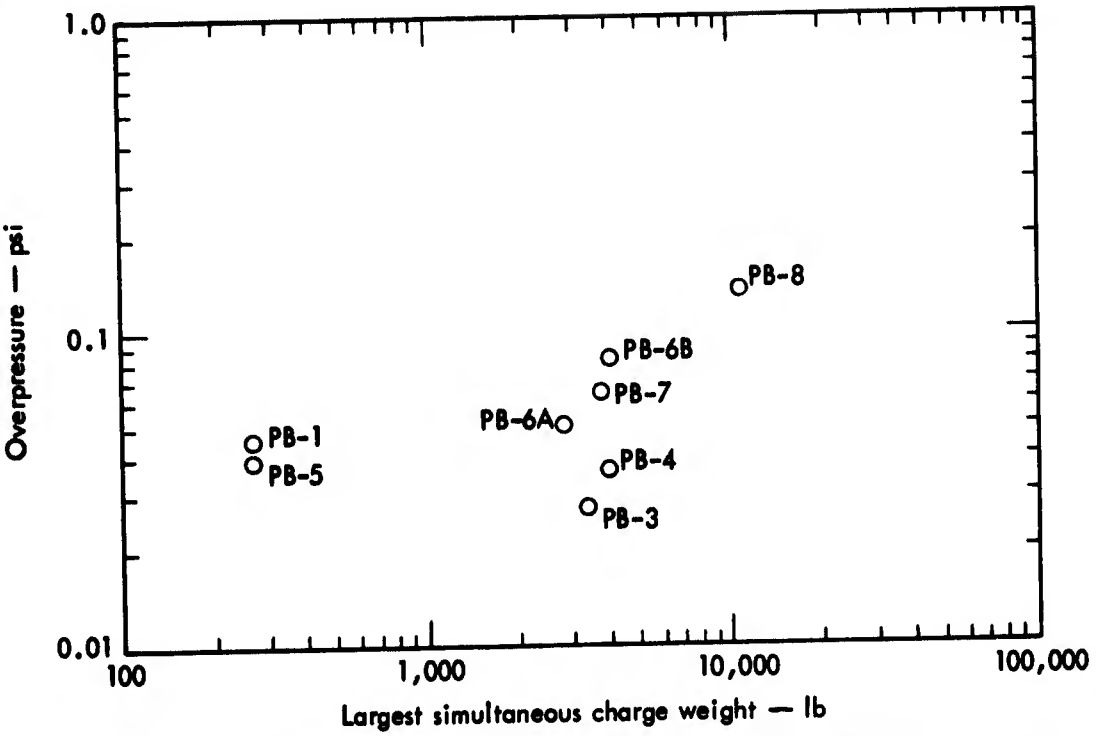

Fig. 8. Peak overpressure vs largest simultaneous charge weight at 1000 ft east.

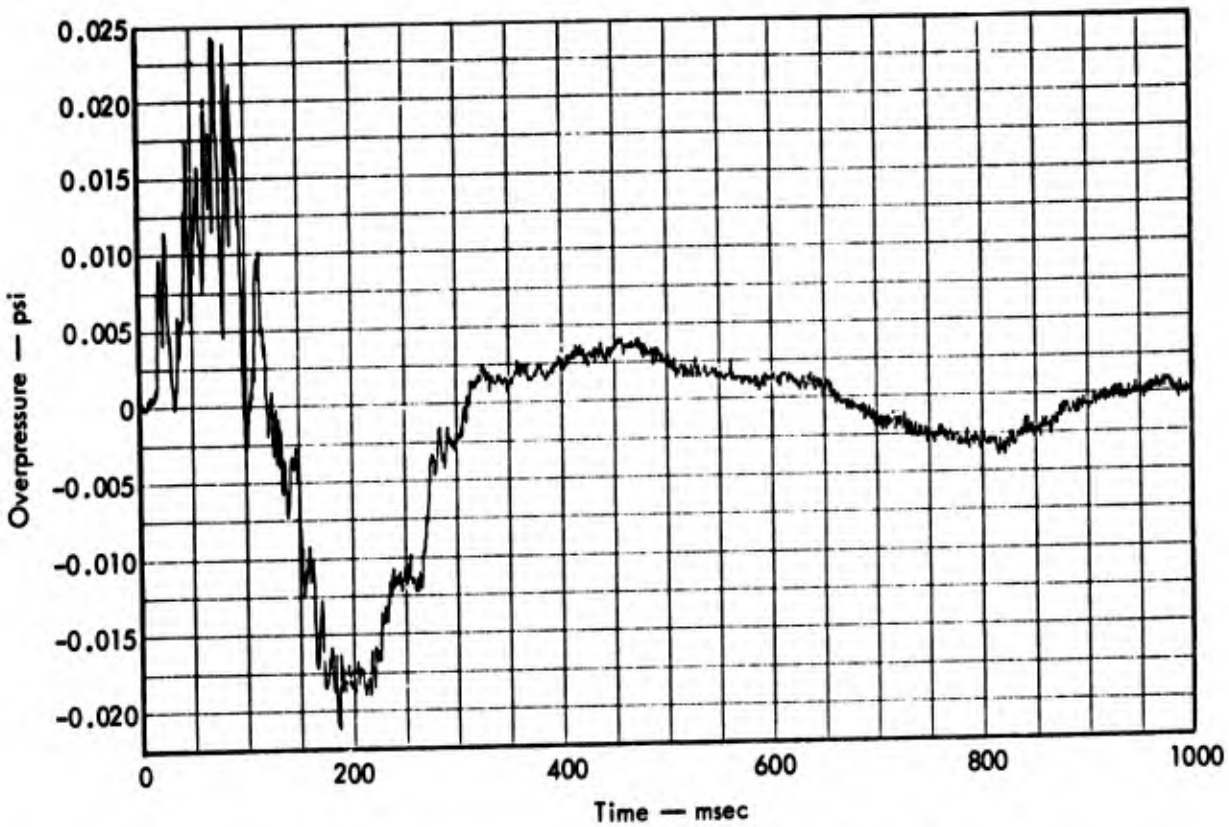

Fig. 9. Overpressure at Gage E-2 from Shot PB-3.

the record obtained at Gage E-2 from Shot PB-3. This wave, however, does not appear to have been the case for the majority of the detonations.

The peak overpressures from some of the detonations appear to have been caused by the detonating cord on the surface instead of the main charges. This is apparent in the records in which the peak overpressure was caused by a single high-frequency pulse. Because of the high frequency of these pulses, it is unlikely that they were caused by enhancement from several charges. It is more likely that they were caused by either detonating cord or a single charge from an array.

The above can best be illustrated by comparing the results of Shot PB-1 with the records from a detonating cord test and a single-charge detonation. Figure 10 gives a plan view of this shot. Figure 11 shows the overpressure time history obtained at Station E-2, which was located approximately 1300 ft east of the shot along the center line. Figures 12 and 13 are the results measured at the same gage of a detonating cord test and a single-charge detonation, respectively. The detonating cord test was a 200-ft piece of 30-grain detonating cord perpendicular to the center line, similar to that used to detonate the PB-1 presplit line. The single charge was Hole 24 of

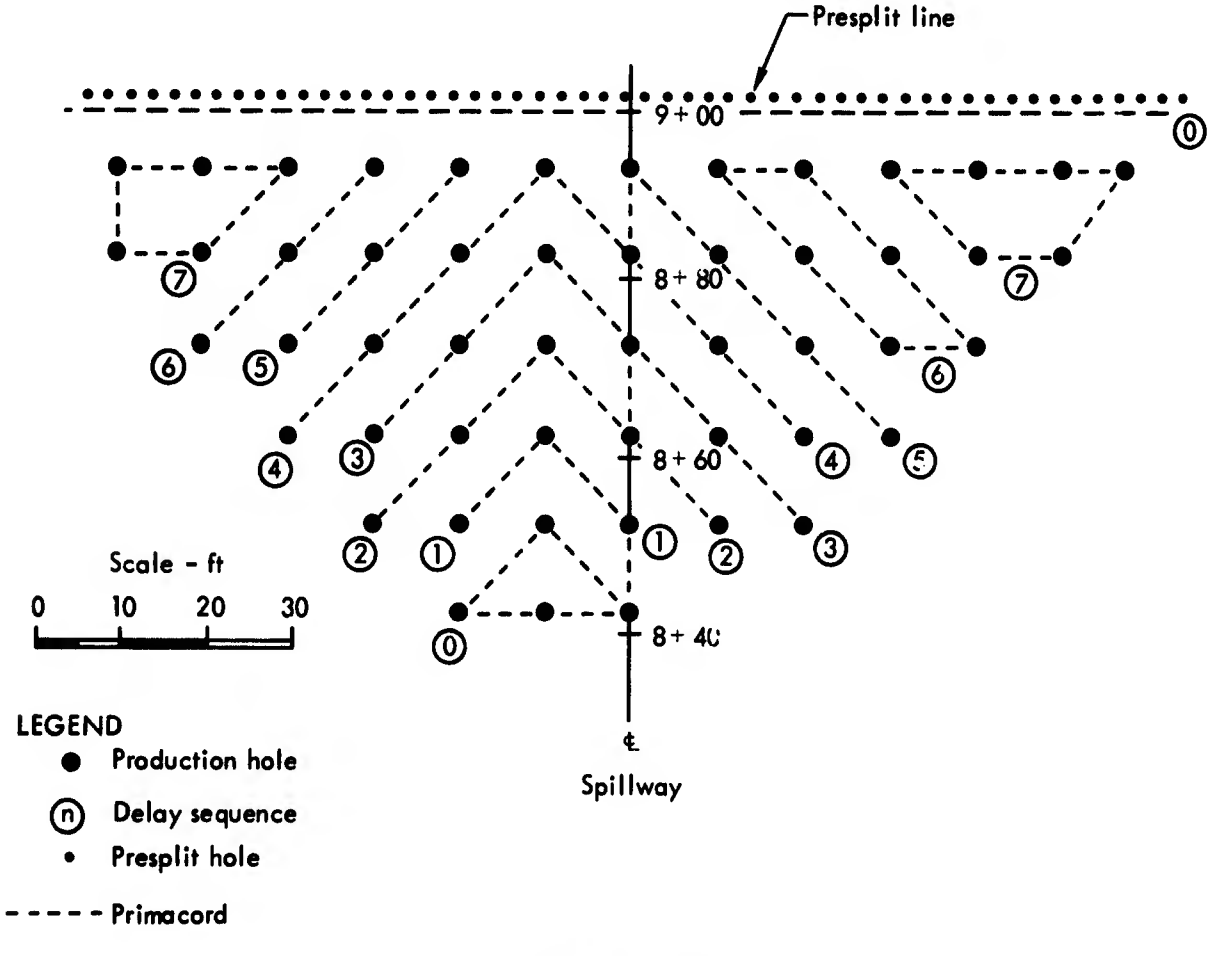

Fig. 10. Plan view of PB-1.

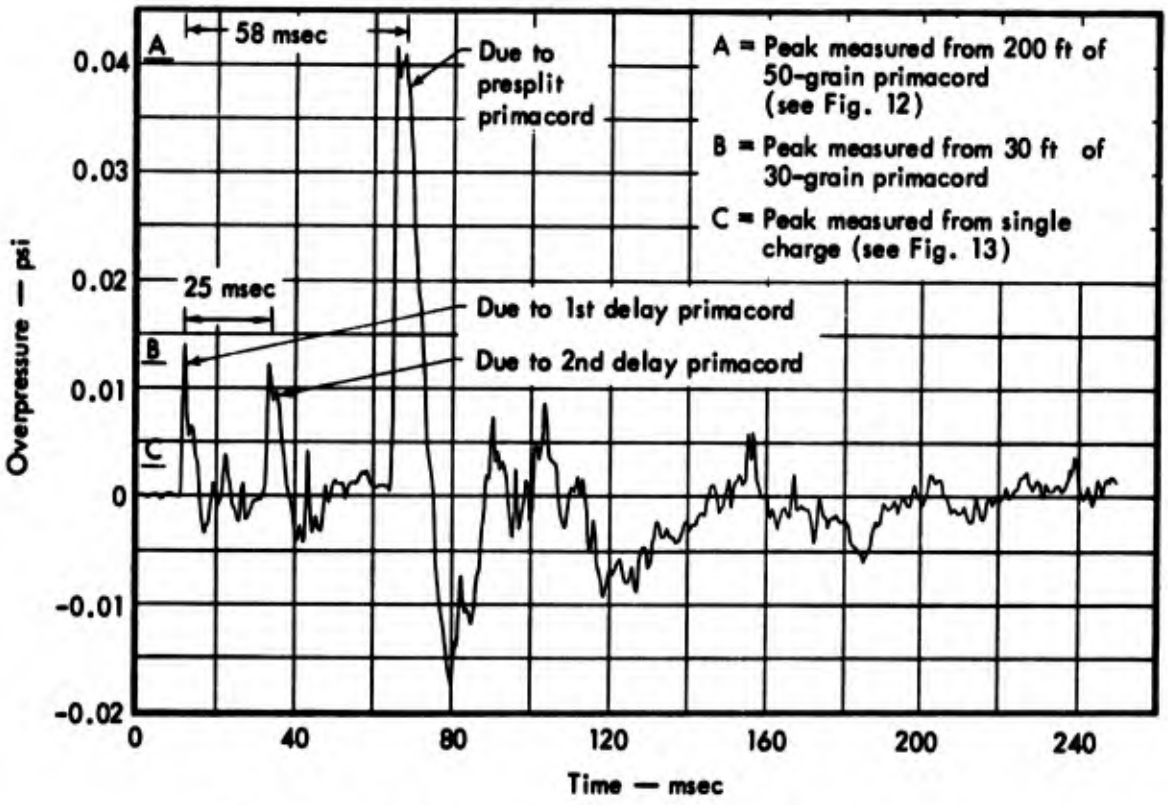

Fig. 11. Overpressure at Gage E-2 from Shot PB-1.

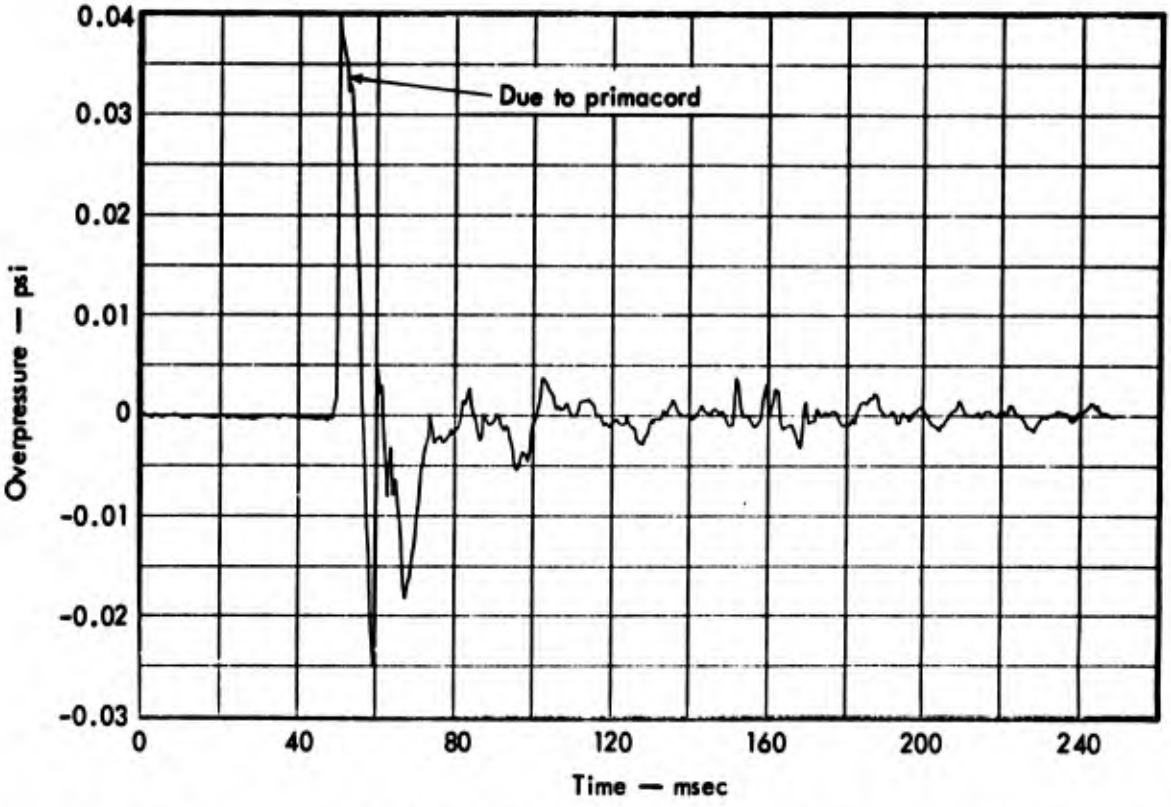

Fig. 12. Overpressure at Gage E-2 from 200 ft of detonating cord perpendicular to the spillway center line.

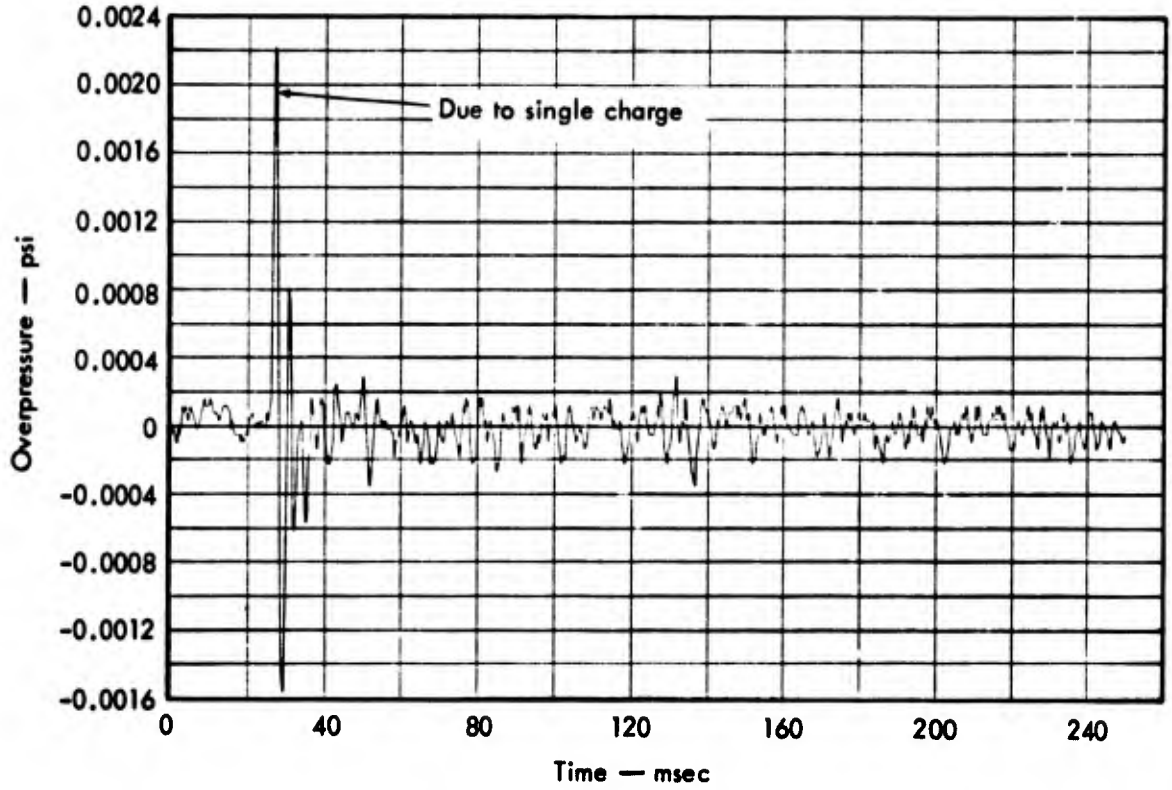

Fig. 13. Overpressure at Gage E-2 from single charge.

the PB-1 array, which had failed to detonate during the PB-1 shot. It can be considered a typical charge for this analysis. These figures were analyzed as follows:

The small triangle containing four charges at the front of the array (see Fig. 10) was detonated at the same time as the presplit line. These charges were detonated with about 50 ft of detonating cord, and the presplit line was fired with about 140 ft of detonating cord. The two events were separated by about 58 ft. The first delay, located about 10 ft behind the front triangle, was fired approximately 15 msec later. Assuming the airblast pulse travels at 1000 ft/sec (or 1 ft/msec), it would be expected that the pulses would arrive in the following order:

(1) The first pulse to arrive would be that produced by the front triangle of detonating cord, followed closely by four production charge pulses. Because the first delay was 10 ft behind the front triangle and detonated 15 msec* later, the second pulse should arrive about 25 msec after the first pulse.

(2) The presplit line was detonated simultaneously with the front triangle but it was about 58 ft behind the triangle; therefore, its pulse should arrive 58 msec after the first pulse.

These expected arrival times are indicated on Fig. 11. Also indicated are the peaks measured from Figs. 12 and 13, which were caused by 200 ft of 50-grain primacord and an average single charge from the array, and the peak measured

*The nominal delay was 25 msec; however, evidence from high-speed photography shows that the actual delay was about 15 msec.

from another test detonation of 30 ft of 30-grain detonating cord. Note that the peak (as determined by arrival times) that should have been caused by the 50-ft piece of detonating cord has an amplitude that corresponds roughly with the amplitude obtained from the 30-ft test strip of detonating cord. This correspondence is also apparent for the single charges and the longer piece of detonating cord.

Further evidence that the large spike was caused by presplit detonating cord was obtained from the record in the opposite direction (Gage W-1) where the large spike was the first arrival – proving that the peak overpressure was due to the presplit detonating cord. The record from PB-1 can also be compared with similar records from presplit detonations (e.g., PB-2PS, PB-4PS) given in Appendix B.

The results of Shot PB-6A are an example of high-frequency pulses being caused by single-charge stemming failures. Although the record obtained at Gage E-2 had a relatively long negative phase, indicating that the overall shape of the curve was determined by the enhancement of charges and not by detonating cord, the individual high-frequency spikes responsible for the peak measurements were probably caused by premature venting from single charges. This conclusion was arrived at in the following manner.

Because of the design of this array, no one hole should have contributed significantly to the peak overpressure over the others. However, in viewing the PB-6A films, it is apparent that many holes had stemming failures, the worst of which appeared to be Holes 3 and 30 (see Fig. 14). Under ideal conditions each hole was expected to produce a peak vertical spall velocity of about 15 ft/sec, which would cause an expected overpressure at Gage E-2 of 0.003 psi. However, the resultant peak overpressure was measured at 0.058 psi. This would be possible from a single hole if the peak vertical spall velocity was 145 ft/sec, or if a stemming failure caused a gas-vent pulse much higher than expected.

It was originally suspected that the two peaks evident on the record from Gage E-2 (Fig. 15) were caused by the 300 ft of detonating cord detonated instantaneously and the 100 ft detonated 125 msec later. An overpressure of 0.058 psi would not be unreasonable from

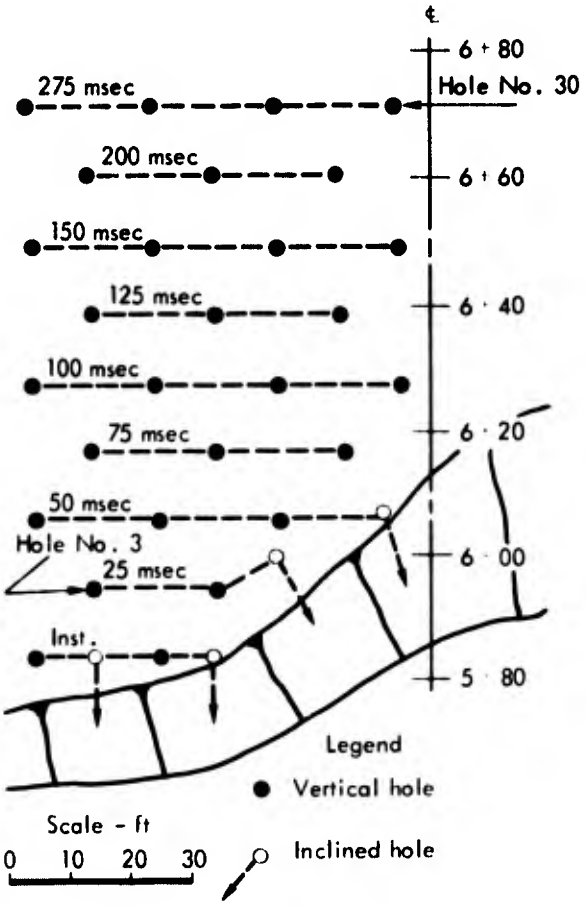

Fig. 14. Plan view of PB-6A.

300 ft of detonating cord, but this 300 ft was not all in one length perpendicular to the center line as were the presplit lines. Instead, the cord was spread out in a series of parallel lines covering about 60 ft along the center line, and should probably be considered as a series of 50-ft pieces spread 11 ft apart.* The first three spikes on the record in Fig. 15 are about 10 msec apart — a fact that would seem to back this statement. Also, if the two delays of primacord, which the films show to have detonated 136 msec apart, were considered to be about 80 ft apart, the second primacord pulse should have arrived 216 msec after the first. But, the two spikes on the record are 320 msec apart. In the opposite direction toward Gage W-2, the first primacord pulse would have traveled 136 ft, or 110 ft past the second piece of primacord before the second piece detonated. Thus, the two pulses would arrive 110 msec apart. On the record for W-2, shown in Fig. 16, the two spikes are 180 msec apart. Hence, primacord cannot be responsible for the two largest spikes on Figs. 15 and 16. Since, the separation of the spikes is dependent on two variables (the time delay and the distance between detonations), these two variables can be computed knowing the

*Note: This 11-ft distance would result in measuring airblast pulses from the detonating cord pieces, which would be separated by about an 11-msec delay. For every 1 ft of distance between detonations, a 1-msec time separation will be recorded between the pressure spikes of each detonation.

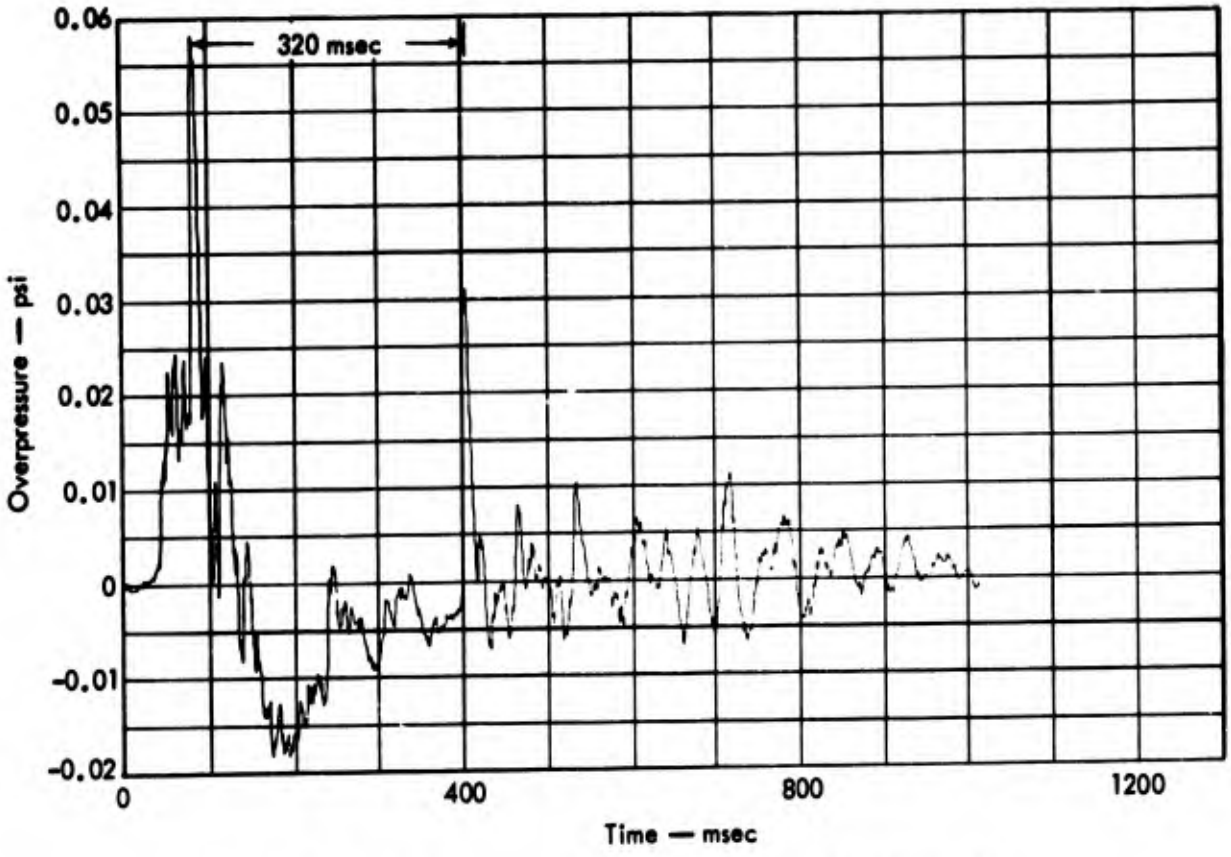

Fig. 15. Overpressure at Gage E-2 from Shot PB-6A.

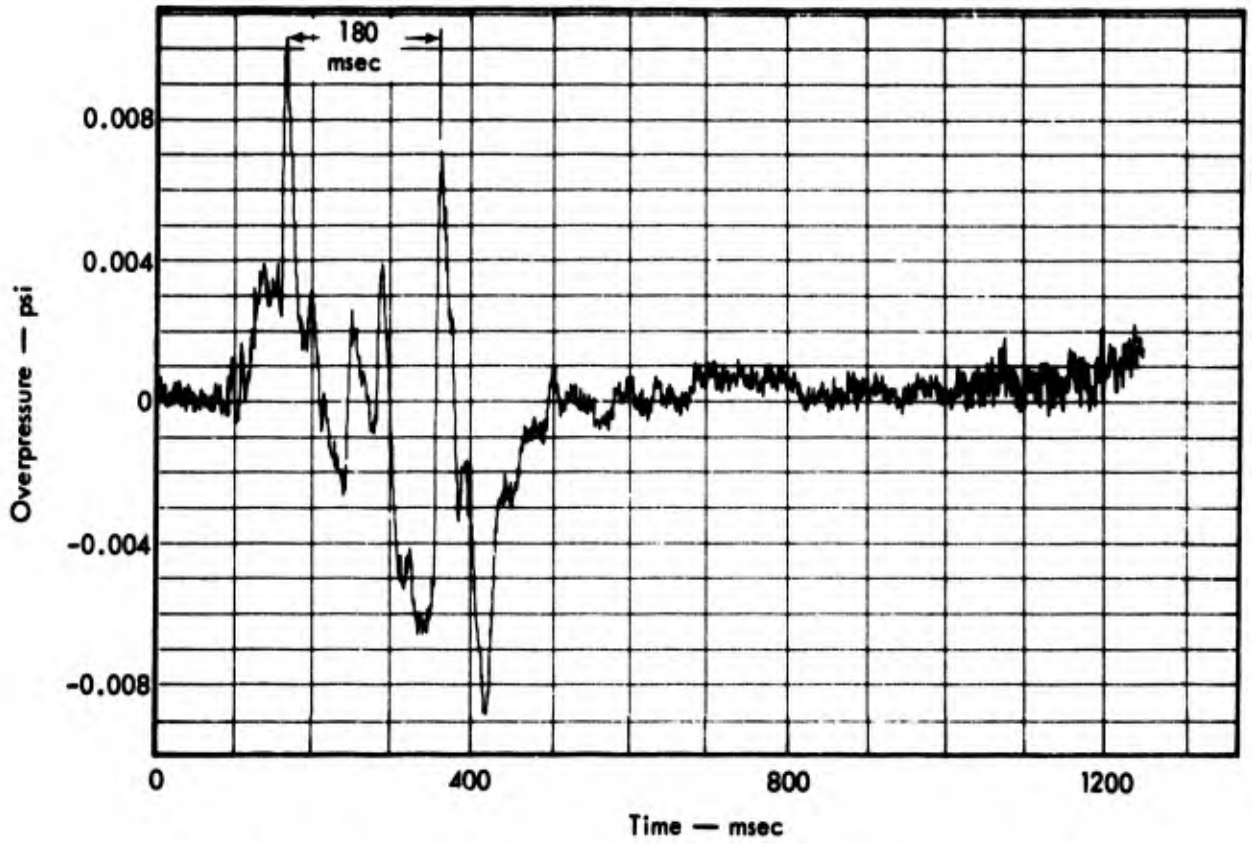

Fig. 16. Overpressure at Gage W-2 from Shot PB-6A.

separations measured in opposite directions:

A + B = 320 ft

A - B = 180 ft

A = 250 msec

B = 70 msec (which is equivalent to a 70-ft separation)

where A is the time delay and B is the linear distance between detonations represented as an equivalent time delay.

Thus, it would seem that the two detonations responsible for the two spikes were 70 ft and 250 msec apart. From the films, Hole 3 seemed to have extra weak stemming as did Hole 30. Along the center line these holes are about 70 ft apart, and, from the films, the two holes detonated 248 msec apart. In addition, Hole 30 was 11 ft and 25 msec behind the instantaneous delay, which would cause the resulting pulse to arrive 36 msec after the first pulse arrival. The first large spike in Fig. 15 arrived 34 msec after the first pulse. It can be concluded that the peak overpressures from the PB-6A detonation were due to the premature venting of Holes 3 and 30.

The third mechanism other than ground-shock-induced pulses that caused peak overpressures on some shots was the dominance of gas-vent-induced airblast pulses. Both PB-6B and PB-8 had larger-than-predicted peak overpressures because, due to the design of the shots, gas-vent-induced airblast became larger than the ground-shock-induced airblast.

Thus, because the peak airblast overpressures listed in Table 3 were caused by four different mechanisms instead of

Table 4. Overpressure suppression factors.

Shot	$\Delta P\text{-}E_{1000}$ (psi)	W-1	W-2	W-3	S-2
PB-1	0.044	2.0	0.75	0.7	0.7
PB-3	.027	0.6	.48	0.7	0.55
PB-4	.036	.67	.37	0.44	0.85
PB-4PS	.075	.20	.07	0.045	0.28
PB-4A	.021	–	–	2.0	1.4
PB-4B&C	.023	–	–	–	–
PB-4D	.026	.31	.26	1.0	1.1
PB-5	.037	.39	.16	0.39	0.6
PB-6APS	.030	.80	.33	–	0.44
PB-6A	.050	.45	.26	–	0.9
PB-4E	.032	.06	.22	–	0.78
PB-6B	.082	.51	.50	–	1.2
PB-7	.067	.36	.26	0.32	0.75
PB-8	0.14	0.045	0.11	0.58	0.58

just ground shock, they did not vary linearly with any of the other parameters.

Table 4 gives the relation of peak overpressures in the other gage directions. They were determined by calculating the ratio of the peak at any gage to the value of the best fit line on the E-direction data at the comparable distance. These ratios are called suppression factors.

The suppression factors for the W- and S-directions generally decreased as the experimental excavation was deepened. As the wall between the shot site and the gages became higher, the peak overpressures became lower relative to the pressure peaks in the direction in which there was no wall.

Another characteristic observed from the airblast data is the method in which the airblast wave spreads out from the source. In the instances in which the detonation site was confined to an area very close to the west wall of the quarry, as shown in Fig. 17, the suppression became greater at the points nearer to the wall than farther away. In other words, positions such as W-1 in Fig. 17 will have a lower suppression factor than will positions such as W-2 if the shot is at A, while for shots farther away from the wall, such as at site B, the suppression factors at positions W-1 and W-2 will be more nearly the same. This indicates that the airblast is directed upward by a

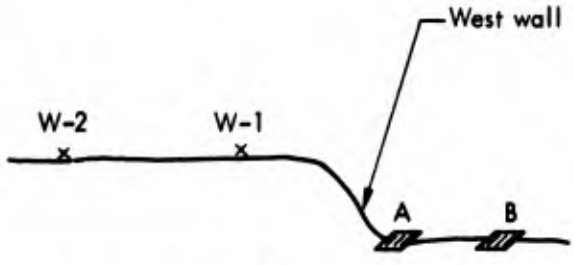

Fig. 17. Shots behind quarry wall.

wall near the side of a detonation and is effectively refracted to positions horizontally directed from the top of the wall, so that at greater distances more of the pressure wave has been refracted back to the ground level. This effect was most evident on Shots PB-4E and PB-8. Both of these were very close to the west wall of the quarry, and the airblast suppression factor was significantly higher at Gage W-2 than at W-1. On the PB-4E shot the pressure amplitude at W-2 was even higher than at W-1.

When possible damage caused by peak overpressure was analyzed, it was noticed that the highest overpressure measured in Justice was 0.0052 psi, which is below the levels indicated in Fig. 2 as causing damage. In the area of the intake structure, the highest overpressure measured was 0.028 psi from Shot PB-6B. This level is near that at which large windows may be expected to break. In general, it was found that for shots the greatest distance at which damage to most windows would begin to occur, using criteria found in Ref. 2, is about 2500 ft. However, this value is the most pessimistic value, because as discussed earlier those criteria may be somewhat conservative.

IMPULSE

The overpressure time history records were integrated with respect to time, using computer techniques to obtain plots of impulse vs time for each record. Peak values were read off these curves and used to obtain peak impulse values at 1000 ft east ($I\text{-}E_{1000}$) and suppression factors for the west and south directions. These values were determined in the same manner as similar peak overpressure values in Tables 3 and 4. The results of this impulse analysis are listed in Table 5.

Figures 18 and 19 are plots of $I\text{-}E_{1000}$ against total yield and largest simultaneous yield. These can be compared to similar plots of peak overpressure in Figs. 7 and 8. The plots of impulse data seem to be somewhat more linear, probably because individual spikes do not

Table 5. Summary of impulse parameters.

Shot	Total yield (lb)	LSY (lb)	Slope b (r^{-b})	$I\text{-}E_{1000}$ (psi-sec) $_P$	W-1	W-2
PB-1	1,150	260	0.718	0.00035	1.15	0.3
PB-3	3,380	3,380	1.29	.0017	0.218	.357
PB-4	20,000	4,000	1.26	.0023	–	–
PB-5	1,188	258	1.21	.00032	0.968	.328
PB-6A	15,350	2,868	1.26	.0016	0.468	.333
PB-6B	8,600[a]	3,993	1.06	.0024	0.583	.421
PB-7	19,950[a]	3,700	0.907	.0025	0.68	.53
PB-8	32,100[a]	10,990	1.56	0.0070	–	0.120

[a]Slurry.

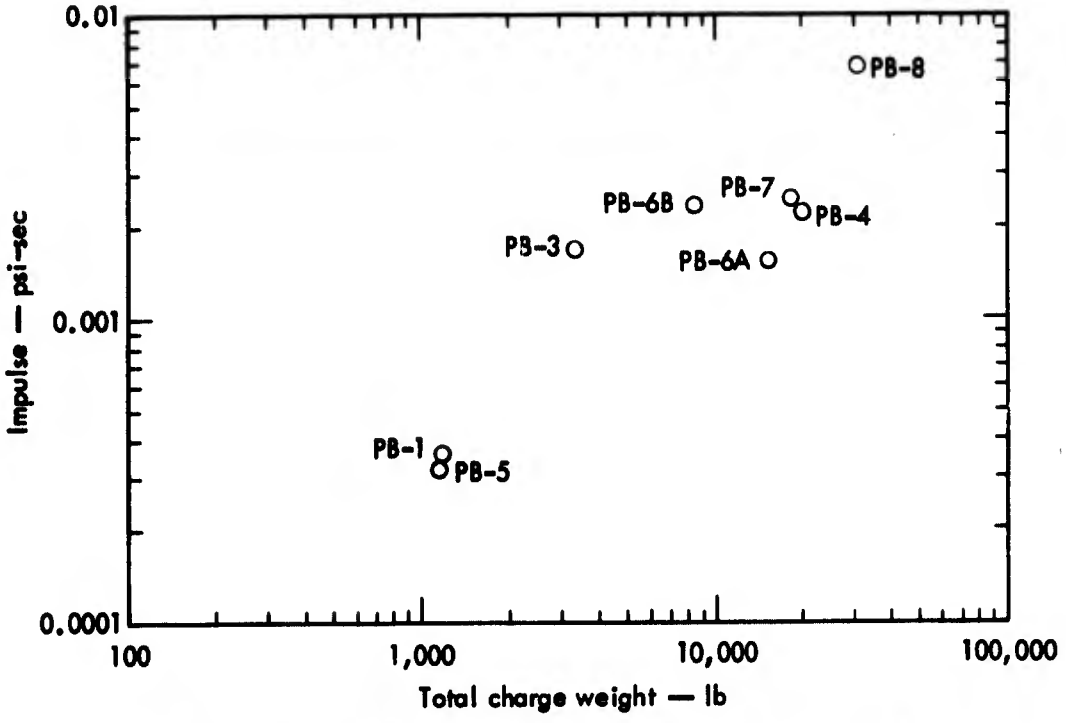

Fig. 18. Impulse vs total charge weight at 1000 ft east.

contribute as significantly to impulse as they do to overpressure. Whereas high-frequency spikes resulting from primacord or single-hole stemming failures cause the peak overpressures, they are only an integral part of the total impulse curve.

The suppression factors listed in Table 5 are generally larger than

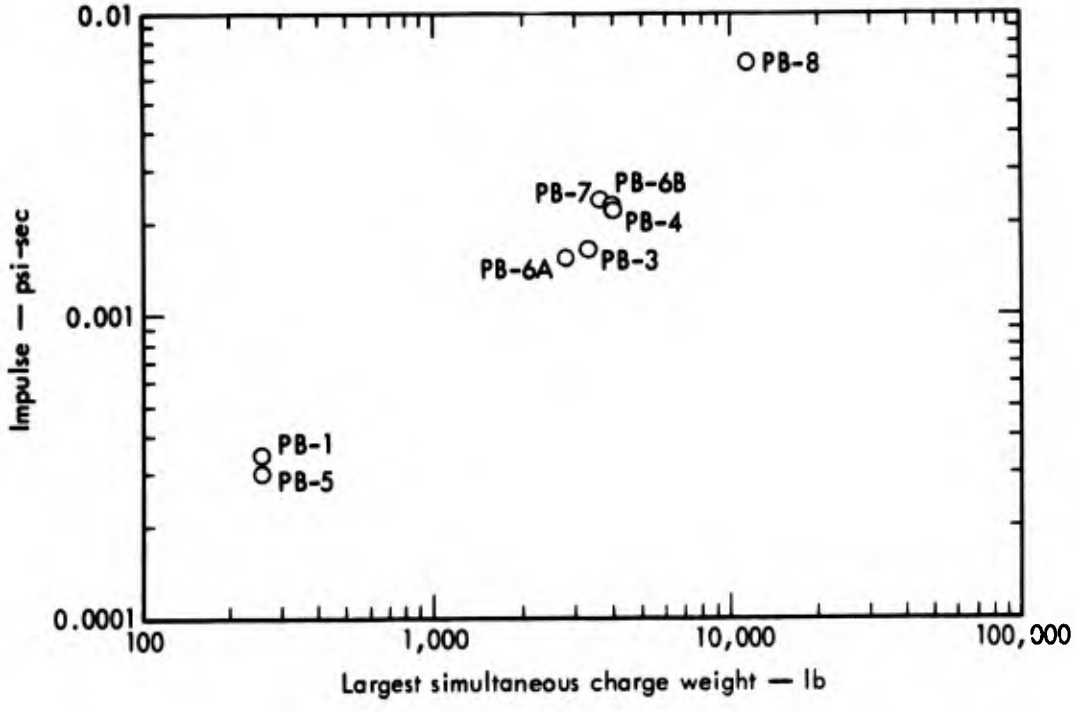

Fig. 19. Impulse vs largest simultaneous charge weight at 1000 ft east.

Table 6. Comparison of results and predictions where possible main charge overpressure is considered along with peak overpressure. (pressures in psi).

Shot	Predicted overpressure at Station E-2[a]	Measured values	
		Possible main charge overpressure[b]	Peak overpressure
PB-1	0.00759	0.0080	0.0368
PB-3	0.0438	0.0240	0.0220
PB-4	0.0260	0.0302	0.0302
PB-5	0.0152	0.0120	0.0386
PB-6A	0.0360	0.0240	0.058
PB-6B	0.0237	0.0260	0.0738
PB-7	0.0523	0.0340	0.0615
PB-8	0.104	0.112	0.113

[a]These predictions are made by the method described in Ref. 6 with additional assumptions as described in the text.

[b]These values are interpreted from the records by identifying and ignoring peak values assumed to be due to primacord on ground surface or early stemming failures.

comparable peak overpressure suppression factors. Thus, topographic factors were less effective in reducing impulse than in reducing peak overpressures.

PREDICTIONS

Predicted values were compared with actual measured values to determine whether present prediction methods are reliable enough to use for predicting overpressures from future detonations of the type used in Project R. D. BAILEY.

Because of exaggerated overpressures due to primacord and weak stemming, it had originally appeared that predictions were not very accurate. However, ignoring primacord and weak stemming spikes, the overpressure that could be said to have been caused by the main production charges was quite close to predictions. As can be seen in Table 6, predictions for the peak overpressure at Gage E-2* varied no more than a factor of 2 from what appears to be the possible main charge overpressure. Of course, the prediction method used was subject to numerous assumptions.

For the arrays used in this project, the Theoretical Method described in Ref. 6 was the best prediction method available, but it was not necessarily meant to be used for arrays with multiple delays and as a result, several assumptions had to be made. First, it was assumed that the material being blasted would produce the same peak vertical spall velocity as did experimental events in rock and other unsaturated media with the same scaled depth of burst. The material at the project site may have been weaker than the rock used to obtain

*Predictions were made for the resulting overpressure at Gage E-2 because the gage had an uninhibited line-of-sight to the shot area.

Table 7. Comparison of results and predictions made using EM 1110-2-3800.[7]

Shot	Distance to Station E-2 (ft)	Largest simultaneous yield (lb)	Scaled distance ($ft/lb^{1/3}$)	Measured peak overpressure (psi)	Predicted overpressure by EM 1110-2-3800 (psi)	
					$DOB/W^{1/3} = 1.0$	$DOB/W^{1/3} = 1.5$
PB-1	1,350	260	212	0.0368	0.073	0.0010
PB-3	1,204	3,380	80	.0220	.019	.0029
PB-4	1,200	4,000	76	.0302	.020	.0031
PB-5	960	258	151	.0386	.0094	.0015
PB-6A	1,020	2,868	72	.0580	.022	.0033
PB-6B	1,100	3,993	69	.0738	.022	.0033
PB-7	1,080	3,700	70	.0615	.022	.0033
PB-8	1,160	10,990	52	0.113	0.031	0.0046

the experimental results, and thus it would produce a lower spall velocity. This could be more accurately determined if a tensile strength test were performed on the in situ material. Also, it was assumed that the depth of burst of each charge was measured to the center of the charge column, which may not be an accurate depth for large length-to-diameter ratio charges. In determining the amount of reinforcement caused by charges in the same row, it was assumed that all charges in a row that were supposed to detonate simultaneously actually did detonate simultaneously. This simultaneous detonation was not the case for rows in which each charge had an individual down-hole delay cap.

Another comparison of the R. D. BAILEY peak overpressure measurements with post-facto predictions is provided in Table 7 and Fig. 20. The predictions in Table 7 and the curves in Fig. 20 are taken from Ref. 7 and show the range of peak overpressures expected from quarry blasts. Reference 7 suggests that the presence of exposed detonating cord or the lack of stemming can increase peak overpressures by a factor

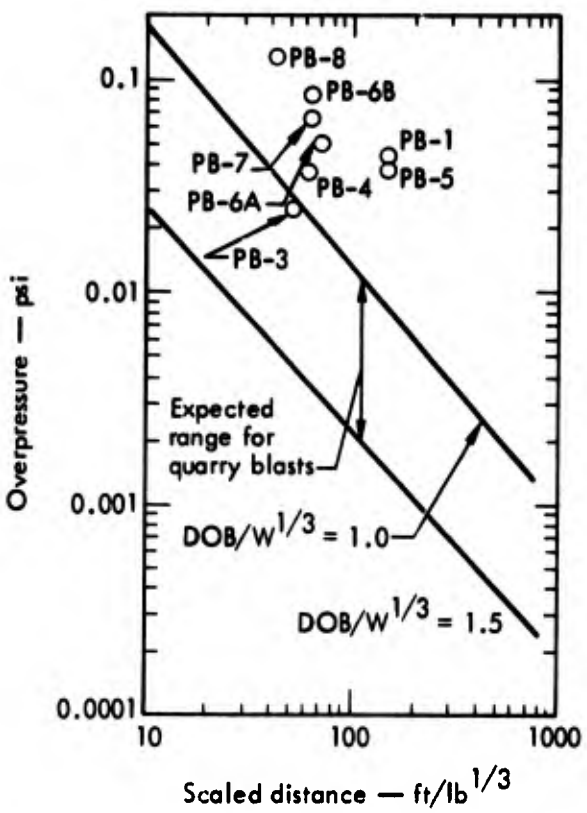

Fig. 20. Comparison of scaled overpressure measurements with post-facto predictions based on EM 1110-2-3800.[7]

of 10 or more over those given by the prediction curves. The R. D. BAILEY measurements were scaled according to the method given in Ref. 7 and plotted in Fig. 20. It is not surprising that these scaled measurements lie above the prediction curves because exposed detonating cord was employed on all the blasts and stemming failures did occur on some.

Tests of electric delay caps showed that they varied from their nominal delay period by as much as 280 msec in some cases (see Table 8). Thus, the reinforcement factor due to these charges would not be as great as the predicted value. Finally, it was assumed that, in estimating inter-row reinforcement, the reinforcement factor for any inter-row distance varied linearly from the optimum range reinforcement to the range at which no reinforcement occurs (see Ref. 6). This variation has not as yet been experimentally proven.

All of these assumptions could cause the predictions to be too high or too low, but the predictions made exercising some judgment seem to be applicable for detonations of the type used in this project if detonating cord and weak stemming effects are ignored. An accurate method for taking into account the effects of topographic features on overpressure has not yet been established.

Table 8. Results of millisecond delay cap tests.

Nominal delay	Measured delay (msec)
0	2-msec spread (5 caps), 0-msec spread (5 caps)
25	17.5, 19, 20.5, 31.5
50	29 to 44 msec (5 caps), 5-msec spread (4 caps)
75	29, 43, 62, 66, 71, 78, 79
100	92, 96
125	123, 125, 131
150	152, 157, 160
175	160, 169, 172, 176, 192, 202, 207, 455

Conclusions and Recommendations

From the analysis of the data obtained from Project R. D. BAILEY, several conclusions can be drawn.

As far as further excavation work in the R. D. BAILEY spillway area, detonations similar to those used for this test series should have no detrimental effect on either the intake structure or local residences. The presence of the south wall will suppress airblast in the direction of the intake structure and, if the excavation continues from the east end, the western wall will suppress airblast in the direction of Justice.

A major consideration for future array detonations is the contribution to airblast from detonating cord on the surface. This airblast overpressure source can be eliminated or at least minimized by covering the primacord with dirt, which will effectively nullify any peaks over those expected from the main charges. If covering is not practical, it will be necessary to make more extensive tests on the overpressure from various configurations of detonating cord in order to predict accurately what the primacord contribution will be.

Another factor that caused larger than expected overpressures was the failure of stemming in some of the detonations. Care should be taken on future detonations to insure that holes are properly stemmed so that this contribution to airblast can be minimized.

The prediction methods presently available can be used to predict for similar arrays, but the estimations that must be made to adapt these methods make predictions somewhat unreliable. The large number of variables present in the R. D. BAILEY pilot excavation program make it difficult to determine the effect of such things as explosives type, length-to-diameter ratio of charges, topographic features, wall height, geologic media, and delay pattern on the resulting airblast pulse. Thus, to establish a prediction method for array detonations from these results would take a considerable amount of guesswork. However, it is hoped that the data obtained can be used in conjunction with future experimental results to formulate a prediction method that can be used with confidence in critical situations.

References

1. C. M. Snell and D. L. Oltmans, A Revised Empirical Approach to Airblast Prediction, U.S. Army Engineer Waterways Experiment Station Explosive Excavation Research Laboratory, Livermore, Calif., Rept. TR-39, November 1971.
2. M. Johnson, Explosive Excavation Technology, U.S. Army Engineer Waterways Experiment Station Explosive Excavation Research Laboratory, Livermore, Calif., Rept. TR-21, June 1971.
3. E. Teller, W. K. Talley, G. H. Higgins, and G. W. Johnson, The Constructive Uses of Nuclear Explosives (McGraw-Hill Book Company, New York, 1968), pp. 198-207.
4. B. C. Hughes, Nuclear Construction Engineering Technology, U.S. Army Engineer Waterways Experiment Station Explosive Excavation Research Laboratory, Livermore, Calif., Rept. TR-2, September 1968.
5. G. A. Bollinger, Blast Vibration Analysis (Southern Illinois University Press, Carbondale and Edwardsville, Ill., 1971), p. 103.
6. C. M. Snell, D. L. Oltmans, and E. J. Leahy, Prediction of Airblast Overpressures from Underground Explosions, U.S. Army Engineer Waterways Experiment Station Explosive Excavation Research Laboratory, Livermore, Calif., Rept. TR-7, August 1971.
7. Systematic Drilling and Blasting for Surface Excavations, Dept. of the Army, Office of the Chief of Engineers, Washing[illegible], D.C., Rept. EM 1110-2-3600 (March 1972).

Appendix A
EERL Airblast System Specifications

A. Gages.

Number and Range of Gages: 3 ea ± 0.1 psi, 2 ea ± 0.2 psi, 1 ea ± 0.3 psi, 1 ea ± 0.4 psi, 1 ea ± 1.0 psi.

Type of Gages: Dynasciences Model P7D variable reluctance, diaphragm type, differential pressure transducers.

Sensing: "+" port open to atmosphere; "-" post fitted with damping tube 15 ft long, 0.25-in. diameter, 0.013-in. diameter opening.

Overrange: Gage damage occurs for 200% pressure overrange.

Gage Circuitry: ac bridge consisting of two gage coils and two bridge completion resistors; gage connected to electronics via Belden YR9797 cable.

B. Hard-Wired Electronics.

System: VGM-AF signal conditioner-demodulator (WES-ISD), 3 kHz carrier, 0-10-Vac rms adjustable excitation.

Channels: Eight; all serviced by one oscillator and one power supply.

Output: Typically ± 4-V full-scale with 5-Vac excitation.

Power Requirements: 10-ma current capacity; dc and ac balance, 115-Vac, 60 Hz.

Recording: Oscillograph and/or tape recorder; frequency capability to 1 kHz.

C. Remote Unit Electronics.

System: Dynasciences CD 32 carrier demodulator, 5 kHz carrier, about 5.7-Vac rms excitation.

Channels: Two units.

Output: Typically ± 4-V full scale; 2.5-ma current capability, dc balance.

Power Requirement: 115-Vac, 60 Hz.

Recording: Oscillograph and/or tape recorder and/or high input impedance recorder; frequency capability to 1 kHz.

D. Calibration.

Method: Resistor shunted across one bridge completion resistor produces voltage step equivalent to certain statically applied pressure.

Frequency Response: All components rated to 1 kHz; estimate of overall linearity is ±10%.

Pressure Linearity: ±1% for static positive pressures 0.1 to 1.2 times gage range; ±5% for pressures 0.01 to 0.1 times gage range.

Variability: Static calibration changes less than ±5% over 1 yr.

Appendix B
Airblast Overpressure Records

Figures B1 through B10 are computer plots of airblast overpressure vs time for most of the main production detonations and some presplit detonations as measured at Gage E-2. This gage was located at the control point trailer and had a clear view of the shot area. These plots were obtained by digitizing the analog tape record obtained in the field and analyzing it by computer programming techniques.

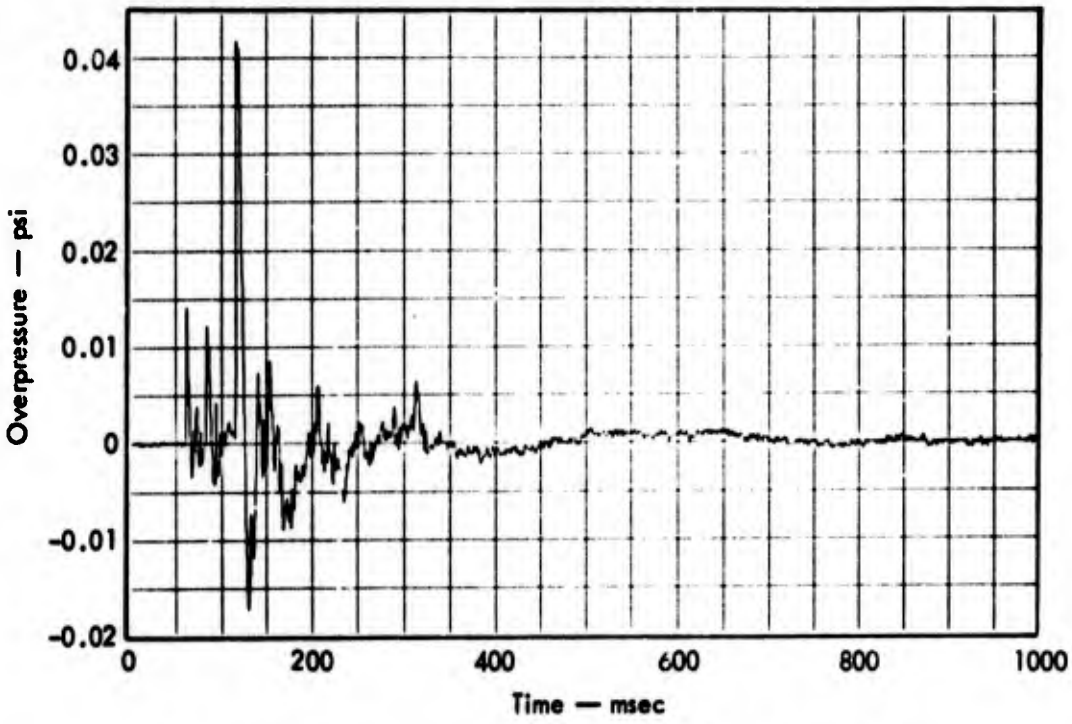

Fig. B1. Overpressure at Gage E-2 from Shot PB-1.

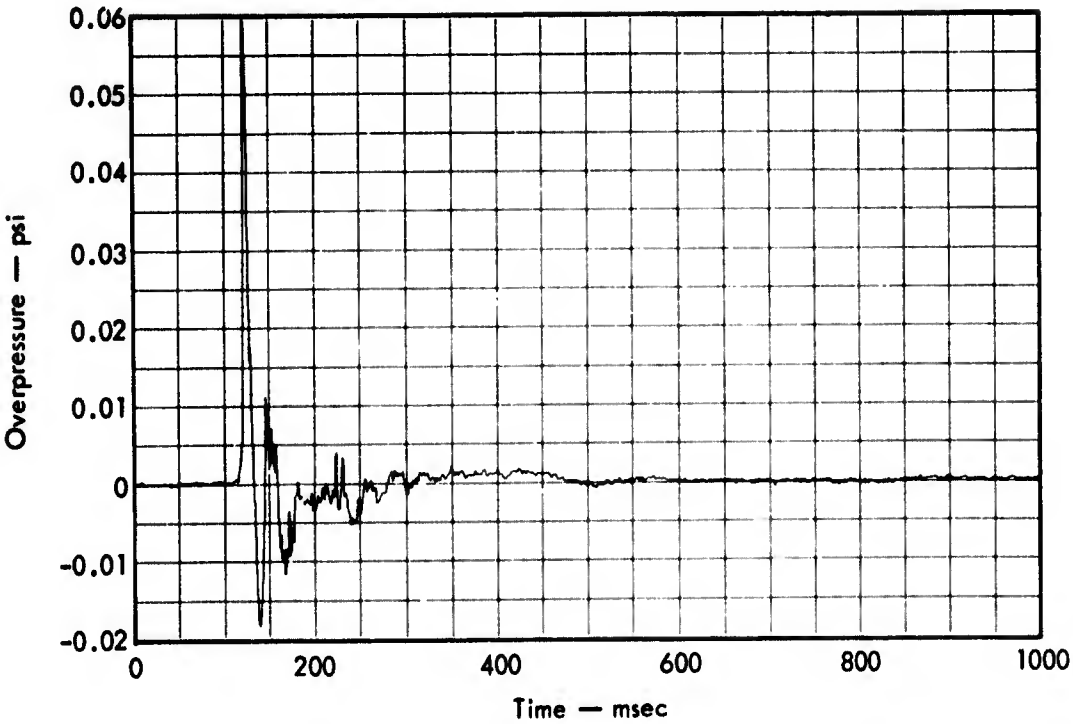

Fig. B2. Overpressure at Gate E-2 from Shot PB-2 presplit.

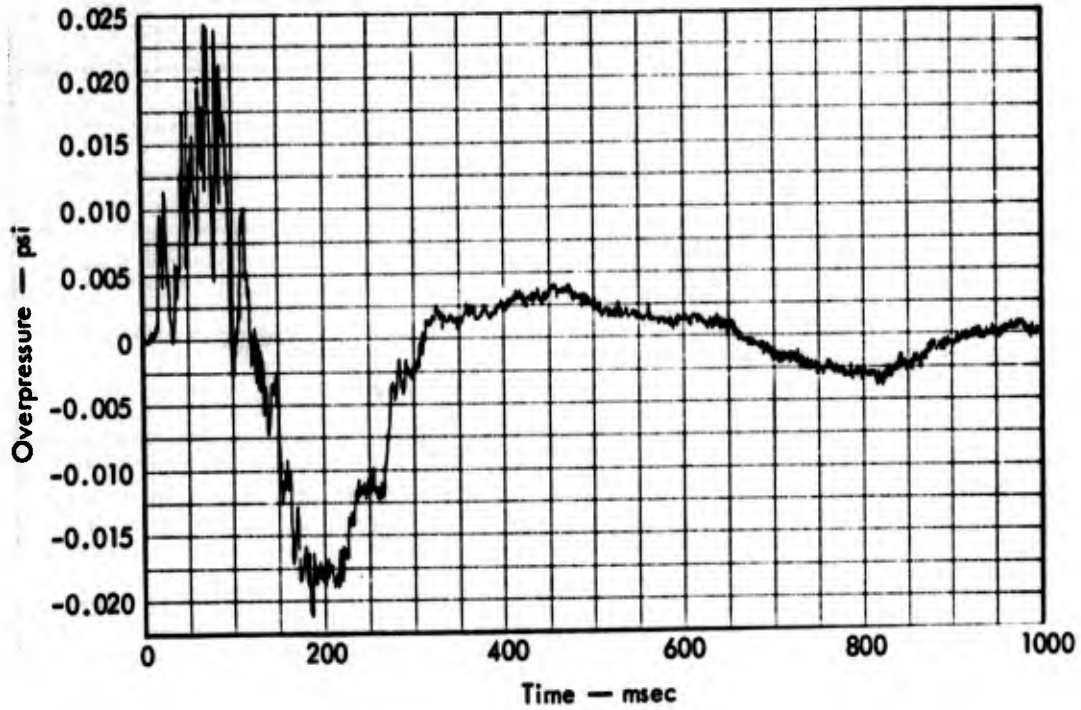

Fig. B3. Overpressure at Gage E-2 from Shot PB-3.

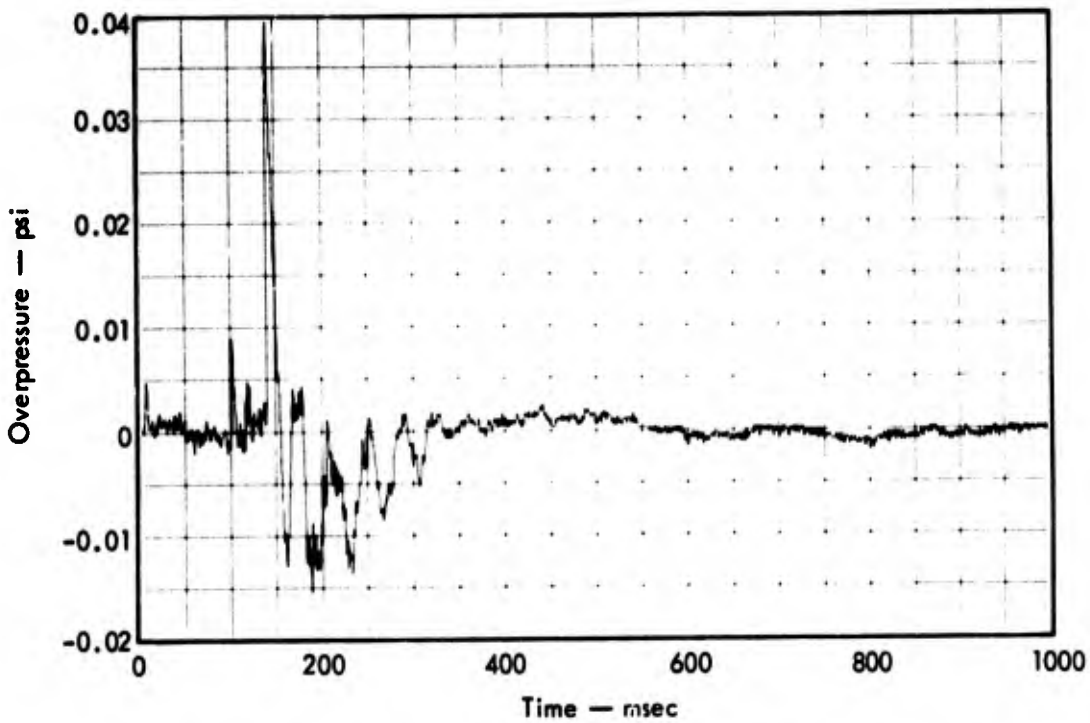

Fig. B4. Overpressure at Gage E-2 from Shot PB-4 presplit.

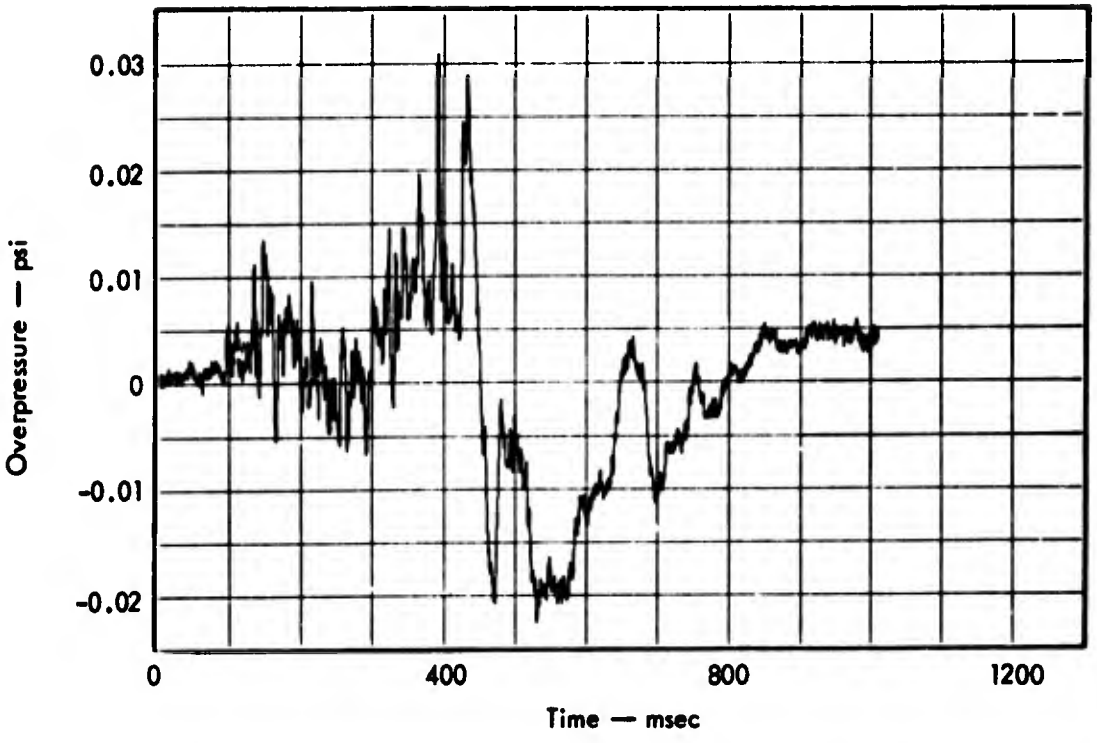

Fig. B5. Overpressure at Gage E-2 from Shot PB-4.

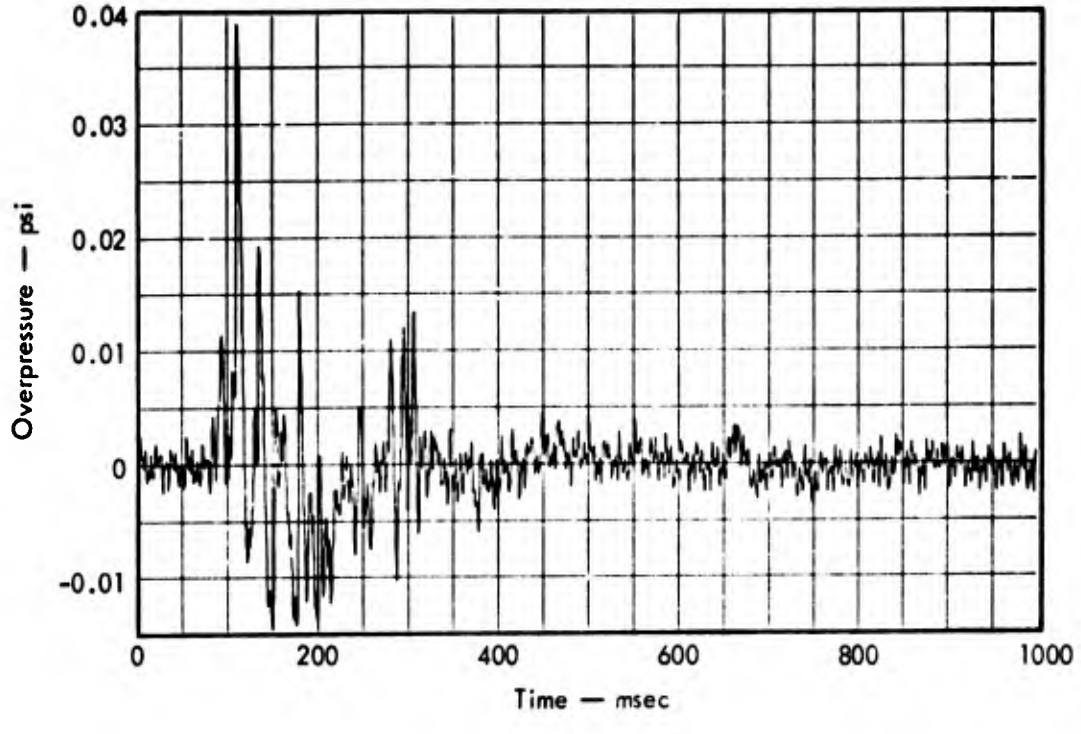

Fig. B6. Overpressure at Gage E-2 from Shot PB-5.

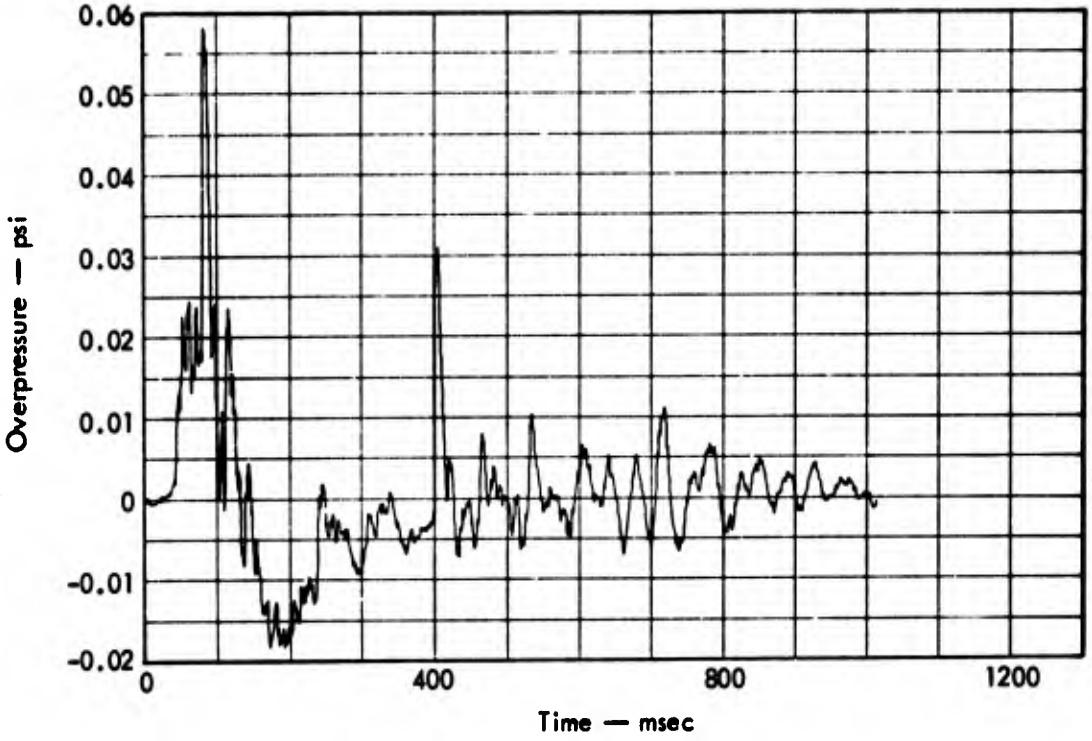

Fig. B7. Overpressure at Gage E-2 from Shot PB-6A.

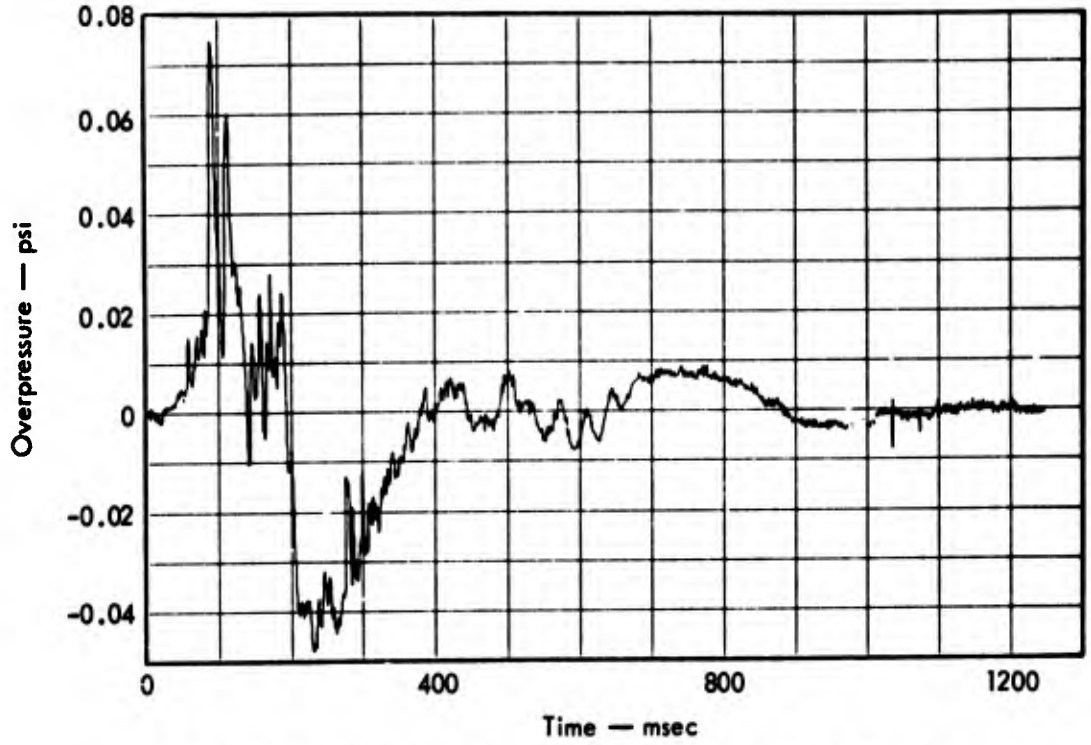

Fig. B8. Overpressure at Gage E-2 from Shot PB-6B.

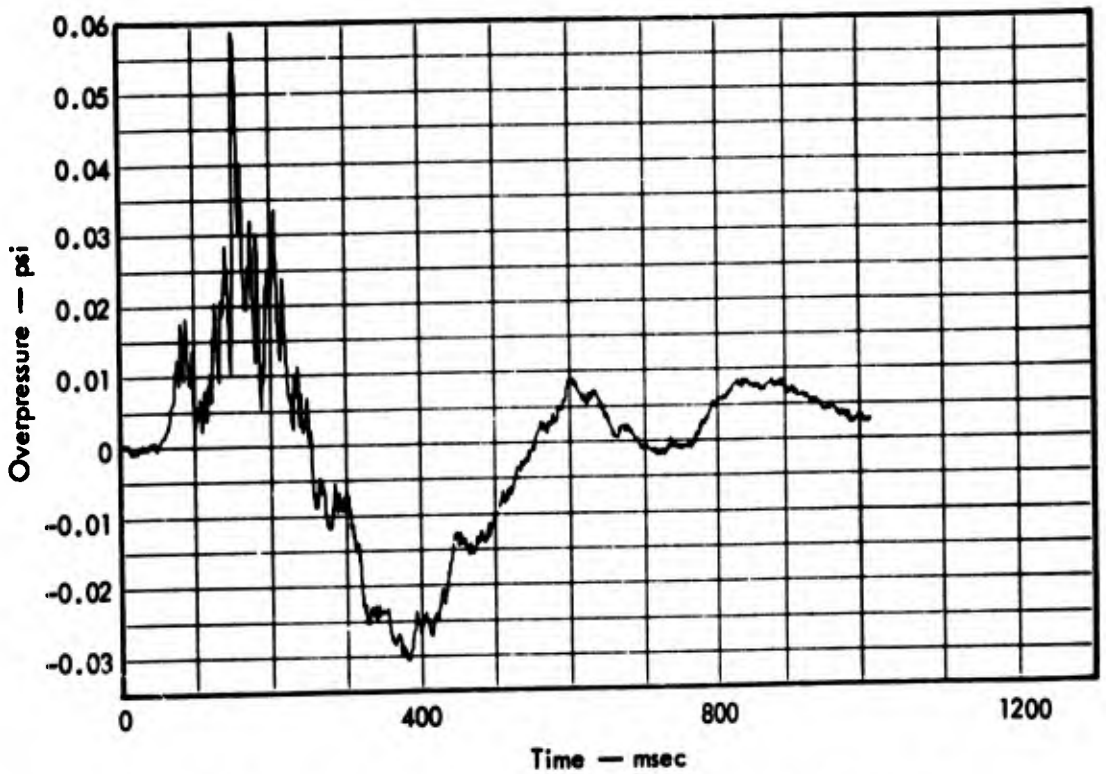

Fig. B9. Overpressure at Gage E-2 from Shot PB-7.

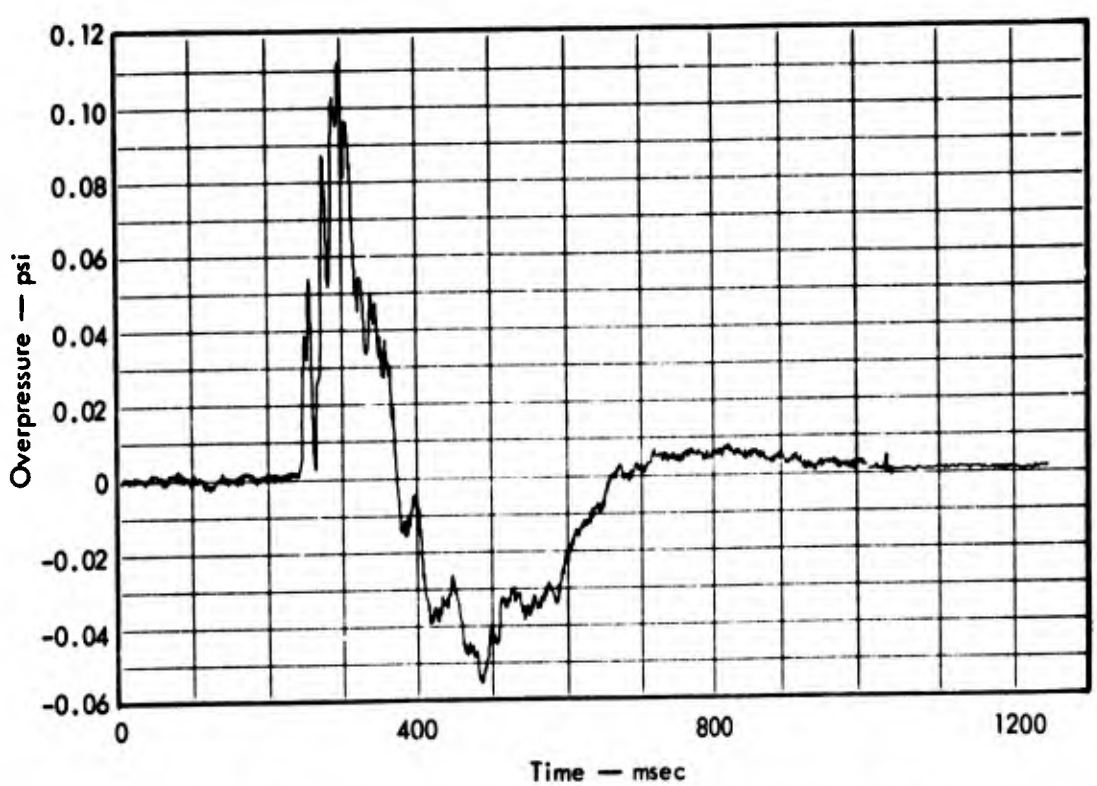

Fig. B10. Overpressure at Gage E-2 from Shot PB-8.

Appendix C
Plots of Airblast Data

Figures C1 through C17 are a set of graphs of peak positive overpressure vs distance for the three directions measured for all shots. In the easterly direction, the airblast pulse encountered almost no opposition on its way to the gages. The westerly direction imposed several hills and much foliage to inhibit the pulse on its way to the gages. This opposition can be seen in the lower levels and steeper slope of the data obtained in that direction. In the southerly direction, Gage S-1 was somewhat hidden from the shot by the south wall of the excavation, whereas S-2 was much farther away and at a higher elevation, which allowed it a clearer view of the shot area. (See Fig. 4 for locations of gages.)

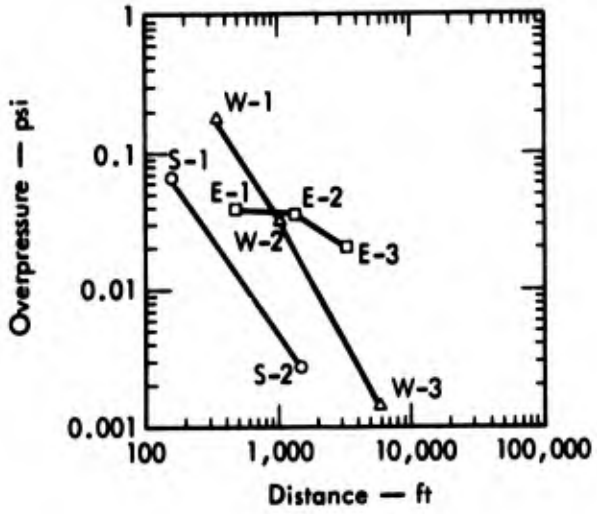

Fig. C1. Peak airblast overpressure vs distance for Shot PB-1.

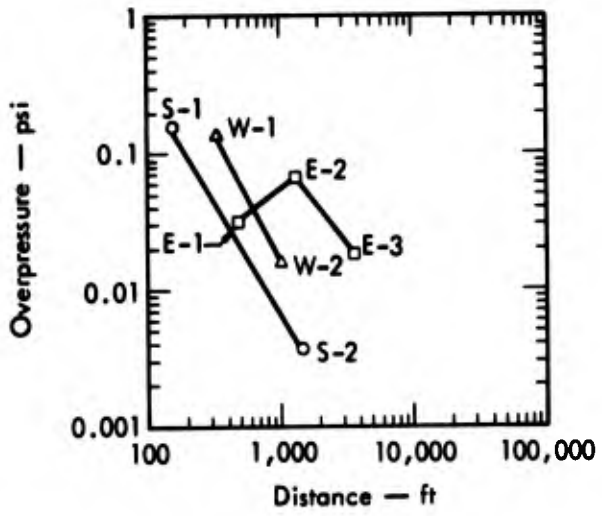

Fig. C2. Peak airblast overpressure vs distance for Shot PB-2 presplit.

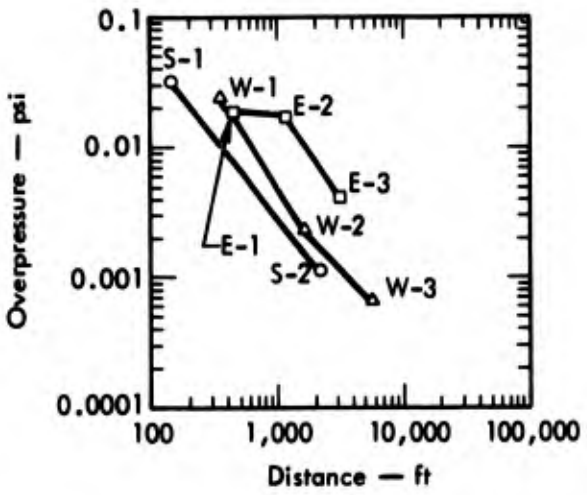

Fig. C3. Peak airblast overpressure vs distance for Shot PB-3 buffer zone.

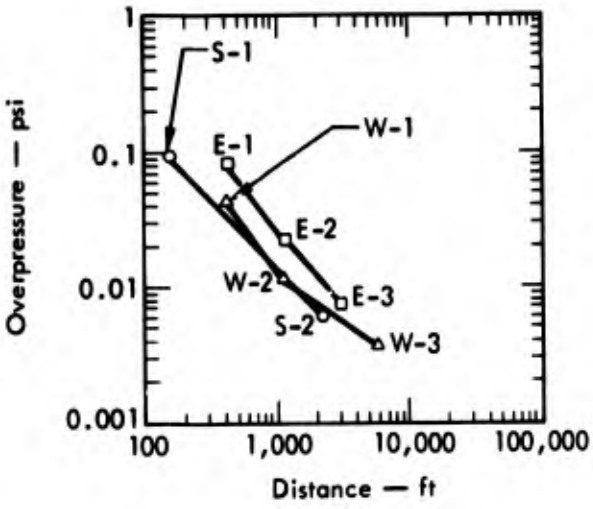

Fig. C4. Peak airblast overpressure vs distance for Shot PB-3.

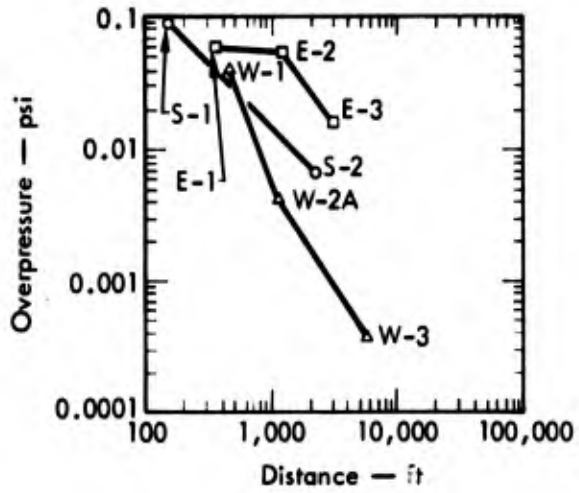

Fig. C5. Peak airblast overpressure vs distance for Shot PB-4 presplit.

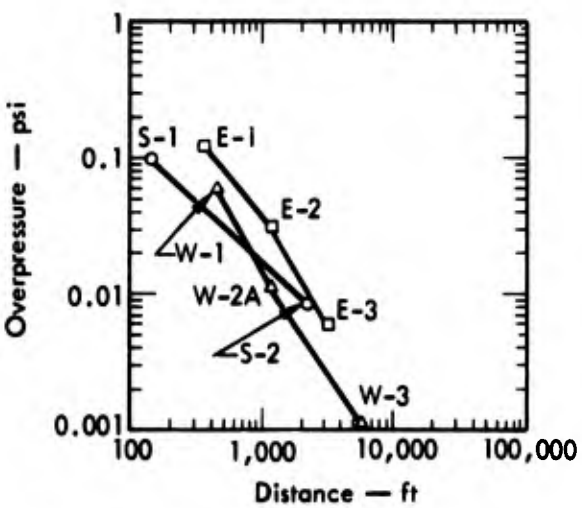

Fig. C6. Peak airblast overpressure vs distance for Shot PB-4.

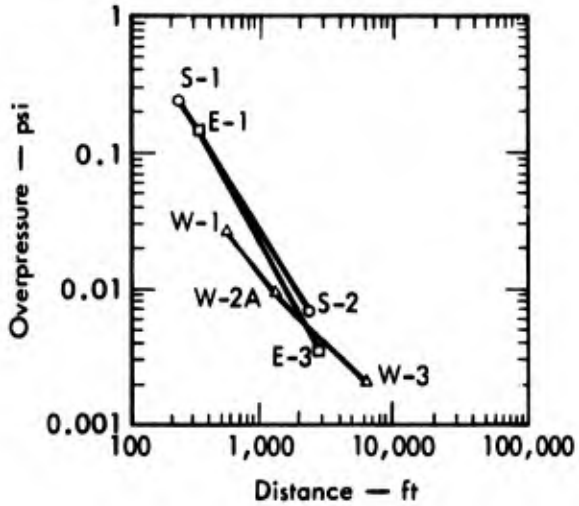

Fig. C7. Peak airblast overpressure vs distance for Shot PB-4A.

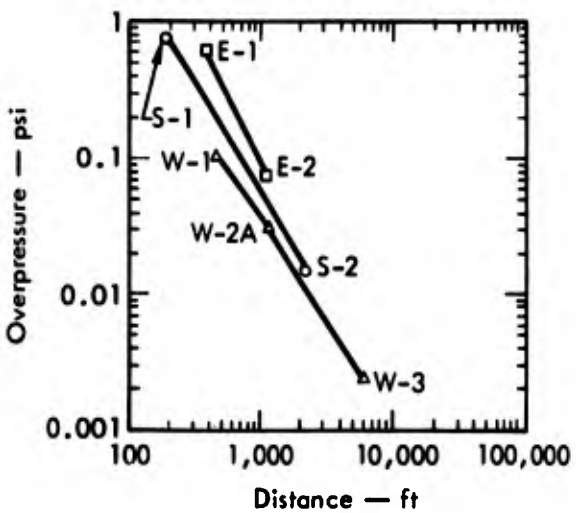

Fig. C8. Peak airblast overpressure vs distance for Shots PB-4B and PB-4C.

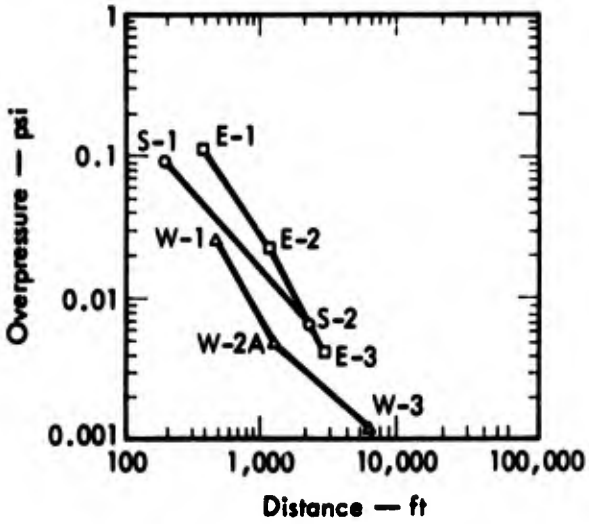

Fig. C9. Peak airblast overpressure vs distance for Shot PB-4D.

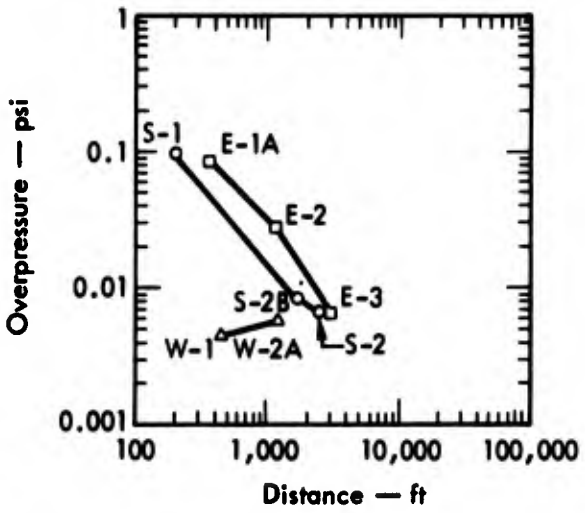

Fig. C11. Peak airblast overpressure vs distance for Shot PB-4E.

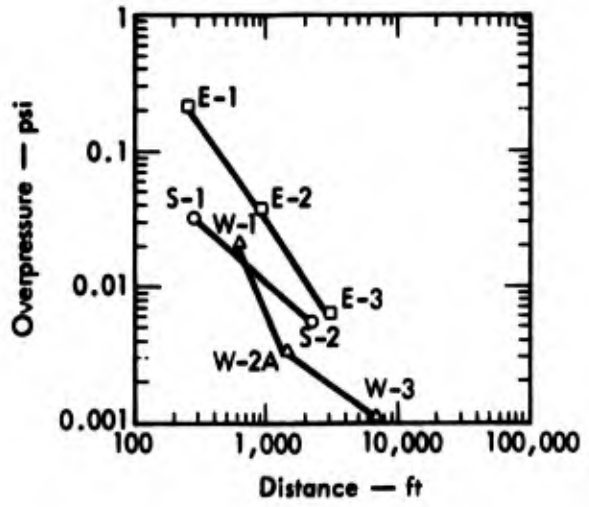

Fig. C10. Peak airblast overpressure vs distance for Shot PB-5.

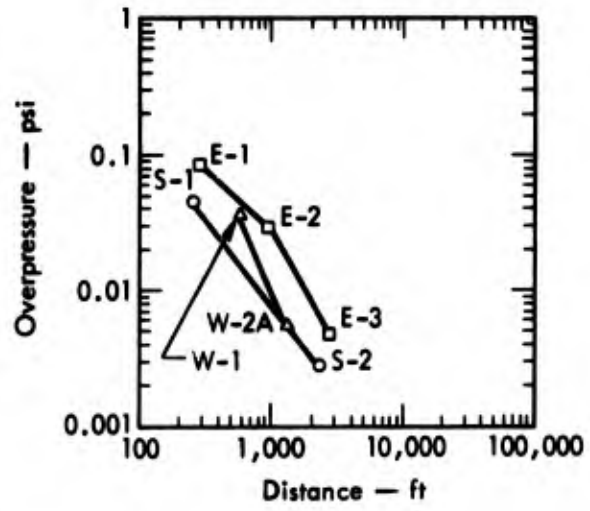

Fig. C12. Peak airblast overpressure vs distance for Shot PB-6A pre-split.

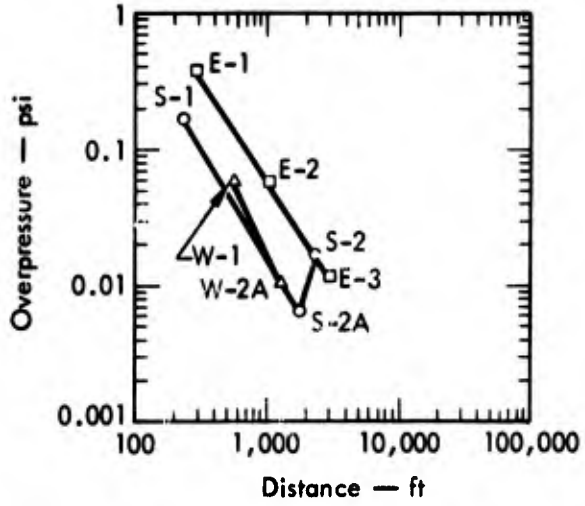

Fig. C13. Peak airblast overpressure vs distance for Shot PB-6A.

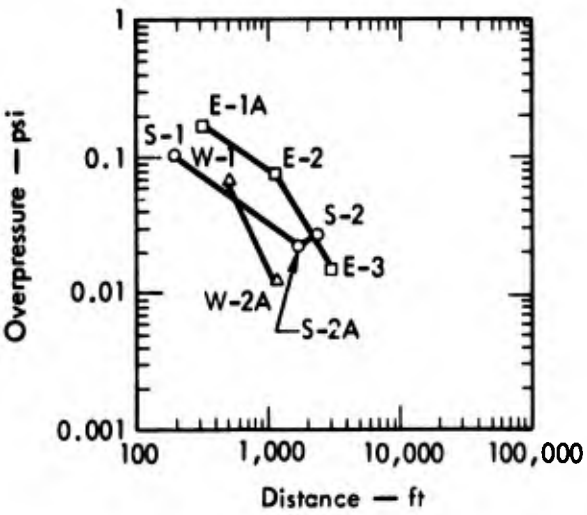

Fig. C14. Peak airblast overpressure vs distance for Shot PB-6B.

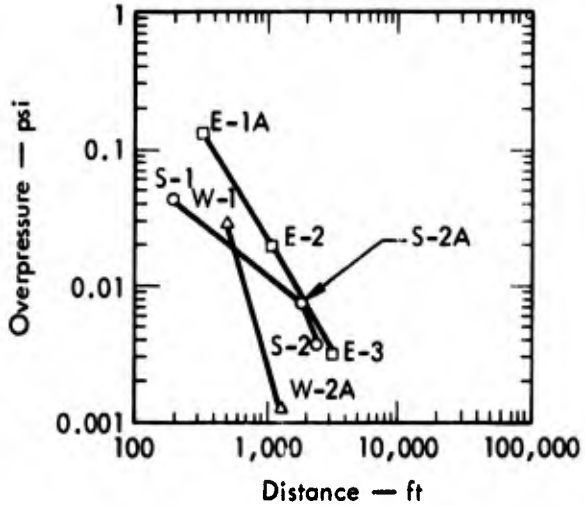

Fig. C15. Peak airblast overpressure vs distance for Shot PB-6C.

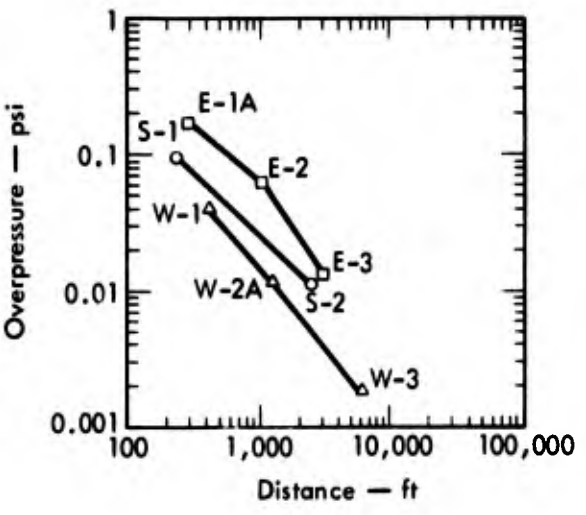

Fig. C16. Peak airblast overpressure vs distance for Shot PB-7.

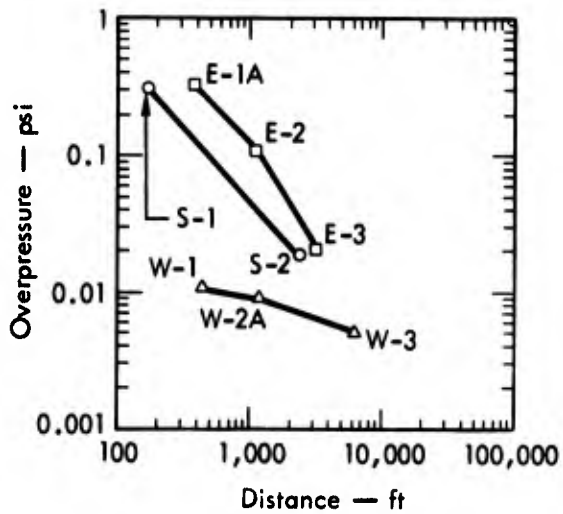

Fig. C17. Peak airblast overpressure vs distance for Shot PB-8.